Aus der Medizinischen Universitätsklinik und Poliklinik Tübingen

Innere Medizin II

(Schwerpunkt: Hämatologie, Onkologie, Klinische Immunologie, Rheumatologie)

In Vitro Effects of the Second-Generation Proteasome Inhibitor Carfilzomib on Human Monocyte-Derived Dendritic Cells

Inaugural-Dissertation
zur Erlangung des Doktorgrades
der Medizin

der Medizinischen Fakultät
der Eberhard Karls Universität
zu Tübingen

vorgelegt von

Dahlfrancis, Philipp Marius Christopher Edward

2020

Dekan:	Professor Dr. I. B. Autenrieth
1. Berichterstatter:	Privatdozent Dr. F. Grünebach
2. Berichterstatter:	Privatdozent Dr. U. Holzer
Tag der Disputation:	16.01.2020

Table of Contents

1. Introduction

1.1 The Immune System

The main purpose of the immune system is to protect the integrity of its host by identifying and eliminating pathogens.
It can be subdivided into the less specialized but immediately reacting innate and the highly specialized but slower-reacting adaptive immune system.

1.1.1 The Innate Immune System

There are different components of the innate immune system. The first line of defence consists of barriers, such as the skin, acidic body fluids or excretion mechanisms. The commensal microbial flora can also be considered part of this. For pathogens which circumvent or withstand these barriers, cells of the innate immune system spring into action, consisting mainly of phagocytes but also a much smaller fraction of natural killer cells (NK).
This second line of defence is able to identify foreign molecules called pathogen-associated molecular patterns (PAMPs) like fungal mannans or bacterial lipopolysaccharide (LPS) via pattern recognition receptors (PRRs) such as toll-like receptors (TLRs), humoral identification or a combination of both (1).
Innate humoral immunity operates in three main ways: the complement system, the acute phase proteins and pro-inflammatory cytokines that the cells of the innate immune system (especially macrophages) secrete. The complement system consists of many different proteins circulating in the blood stream. It has the ability to opsonize (mark for phagocytosis) or lyse pathogens directly, depending on the activated cascade.
Pro-inflammatory cytokines like TNF, IL-1 and IL-6 can cause fever, attract more immune cells and stimulate the production of acute-phase proteins like the C-reactive protein (CRP), which in turn acts as an opsonin and helps to activate the lytic complement cascade (2).

1.1.2 The Adaptive Immune System

Like the innate immune system, the adaptive immune system also has a cellular and a humoral component, both of which are essentially represented by two types of lymphocytes with very distinct roles.
The B lymphocytes (B cells), which can transform into antibody-producing plasma cells, represent the backbone of the humoral component, and the many subsets of T lymphocytes (T cells) make up the cellular component. Both types are created in the bone marrow, but only B cells remain there for maturation, while T cells emigrate to the thymus. In the thymus, T cells undergo processes of positive and negative selection to ensure that they recognize major histocompatibility complex (MHC) molecules with their T cell receptor and that their affinity to self-antigens is sufficiently low.

1.1.3 Antigen-Presenting Cells

The adaptive immune system can reach its full potential by being provided with a specific target. Specialized antigen-presenting cells (APC) are cells capable of incorporating and processing antigens (e. g. pathogens or their fragments) which are then presented on the cell surface via the MHC II protein. Among the specialized APC are B cells, macrophages and dendritic cells (DC). Other cells can only present endogenous antigens (e. g. viral peptides) via MHC I after degradation in the proteasome. Proteasomes are intracellular protein-structures which degrade old or damaged proteins, as well as endogenous antigens.

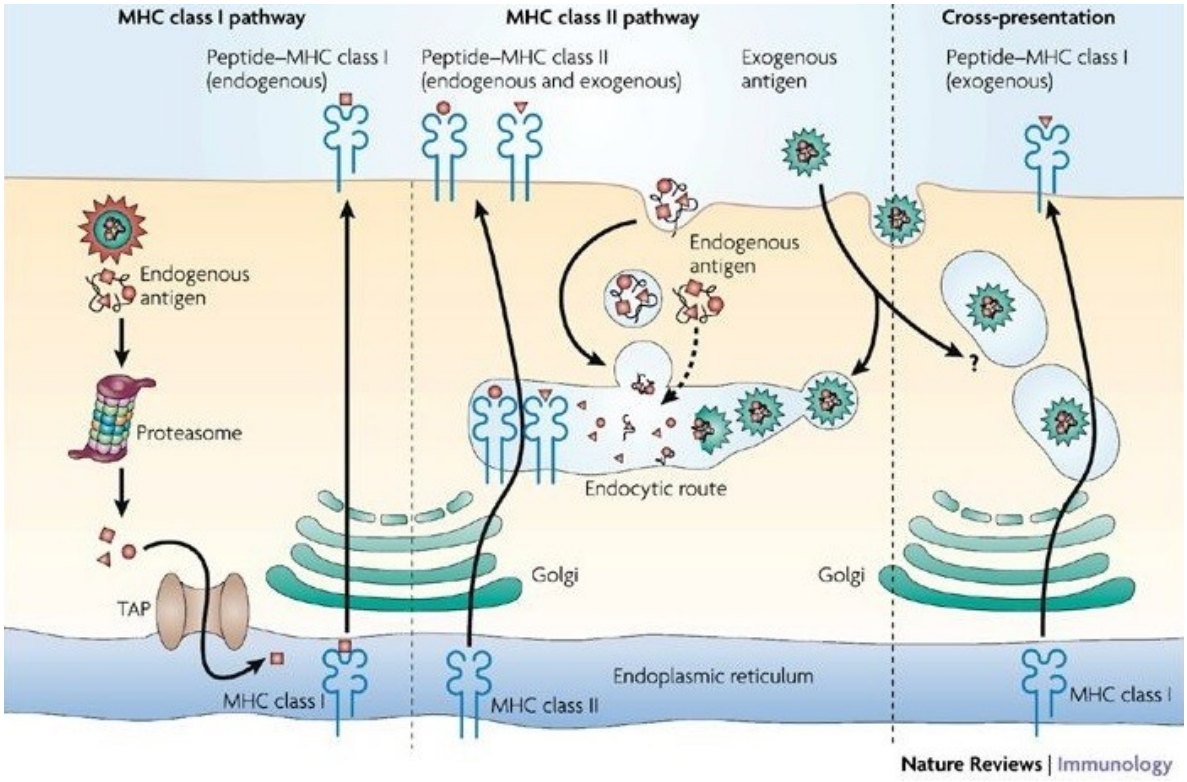

Figure 1.1.3: Modified from "The Antigen-presentation Pathways in DC" (3)

Intracellular antigens are degraded via the proteasome, then transported into the endoplasmatic reticulum where they are loaded onto MHC I proteins. This antigen-loaded MHC I is then sent to the cell membrane to be presented on the cell surface.

Extracellular antigens are incorporated into the cell via endocytosis, then degraded and loaded onto MHC II proteins in the endosome. The antigen-loaded MHC II is then sent to the cell membrane to be presented on the cell surface. Some intracellular proteins are also presented via MHC II.

DC can cross-present extracellular antigens via MHC I. The exact mechanism of this pathway is as of yet unknown.

TAP – transporter associated with antigen processing

Their inhibition causes intracellular protein accumulation and changes to the cellular peptidome (4). DC have the unique ability to present exogenous antigens on both MHC molecules. This is called cross-presentation (5, 6).

1.1.4 T Cell Subsets

Surface molecules are crucial for differentiating cell subsets. Virtually all T cells express the CD3 molecule and the T cell receptor (TCR), but they can be divided into T cells that express CD4, CD8 or neither of the two.

$CD4^+$ T cells include helper T cells (T_h) and regulatory T cells (T_{reg}). Both classes and their respective subclasses are differentiations of the naive $CD4^+$ T cell.

T_h cells have several subsets and promote immunity with their cytokines but every subset also needs a distinct combination of cytokines for their differentiation from the naive $CD4^+$ cell. T_{h1} cells need IL-12 and IFN-γ and have the ability to promote inflammation and cellular immunity. They do so by activating macrophages and cytotoxic $CD8^+$ T cells while suppressing T_{h2} immunity (7). On the other hand, T_{h2} cytokines support humoral immunity by stimulating antibody production and immunoglobulin class switching in B cells.

T_{reg} cells generate immune tolerance by secreting IL-10 and TGF-β as anti-inflammatory cytokines but also need TGF-β along with IL-2 for their formation.

There are also cell contact dependent mechanisms of interaction between T cells and other immune cells, the two most notable examples being the interaction with APC and the interaction with B cells.

To become a T_h cell, the $CD4^+$ T cell engages the MHC II presented antigen with its TCR. However, the result of this alone would be an anergic T cell. The interaction between CD28 on the T cell and the appropriate ligands CD80 and CD86 on the APC surface provides the necessary costimulation (8) (see also figure 1.1.5).

B cells can recognize, incorporate and degrade circulating antigens as well. The presented antigen on the cell surface is then recognized by T follicular helper cells (T_{fh} cells) with an antigen-specific TCR. Upon recognition, the T_{fh} cells express CD40 ligand (CD40L) and secrete IL-21. CD40L binds to the receptor molecule CD40 on B cells and is the requisite co-stimulus for B cell proliferation and differentiation into plasma cells and also memory B cells, which can be activated more quickly, so re-infections with the same pathogen can be fought more efficiently; IL-4 and IL-21

support this effect (9, 10).

$CD8^+$ cells can recognize proteins presented via MHC I on every cell of the organism. When an aberrant cell, virus-infected or neoplastic, expresses proteins that differ from the norm, the $CD8^+$ cell can transform into the cytotoxic T lymphocyte (CTL). This effector cell can secrete IFN-γ along with perforins and granzymes as cytolytic agents to induce apoptosis of the aberrant cell. Additionally, T cells have the ability to engage the CD95 surface molecule with the CD95 ligand which induces programmed cell death (11). After eliminating the threat, homeostasis has to be restored: plasma levels of certain humoral agents and cell counts have to decline. Effector cells go into apoptosis via CD95 ligand binding (12) while memory cells remain in circulation.

1.1.5 Dendritic Cells

Dendritic cells (DC) are specialized APC which can be found in many tissues, especially those that act as a barrier against pathogens. An example would be the Langerhans cells residing mostly in the skin and mucosal tissue. DC were first described as such by Steinman and Cohn in 1973, but their high potential and pivotal role in adaptive immunity was discovered within the following 25 years by Steinman and Banchereau (13, 14).

DC originate from $CD34^+$ progenitor cells in the bone marrow, enter the bloodstream as precursors and have the task of scanning their environment in different tissues for pathogens. They are then called immature DC (iDC), which excel at antigen recognition via PRRs and endocytosis. Having been activated by an antigen or PAMP, iDC migrate to secondary lymphoid organs while processing the antigen. Migration is possible due to an up-regulation of the C-C chemokine receptor type 7 (CCR7), which guides DC to the lymph nodes. During migration, they lose their high potential for antigen recognition and endocytosis while profoundly improving their aptitude for antigen-presentation and co-stimulation. After completing this process they are now called mature DC (mDC). Their main function is to present the processed antigen via MHC and thereby select an appropriate T cell clone for clonal expansion. Once a suitable T cell makes contact with

the MHC presented antigen via its TCR, the mDC can supply the necessary costimulatory surface molecules – especially CD80 and CD86, but also CD83 (15) – as well as supporting cytokines (e. g. IL-12). DC can also be activated by T cells binding to CD40L. This leads to increased expression of costimulatory molecules, secretion of more cytokines and indirectly supports B cell organization (16). Their high potency as APCs results in DC being able to directly prime naive T cells to specific antigens and therefore link innate to adaptive immunity (17).

While mDC can promote immunity, iDC can have the opposite effect, creating immune tolerance. Steinman showed this effect by targeting DC without a maturation adjuvant to suppress type I diabetes in mice (18).

One can differentiate between myeloid and plasmacytoid DC. Myeloid DC have many subsets like the aforementioned Langerhans cells. Plasmacytoid DC look like plasma cells while also having TLRs for antigen recognition. After stimulation they secrete large amounts IFN-α and IFN-β (19).

A special subset of DC are the monocyte-derived DC (MoDC). They can be generated *in vitro* by subjecting $CD14^+$ monocytes to the cytokines IL-4 and GM-CSF. Their maturation can be induced via different stimuli like TNF or LPS.

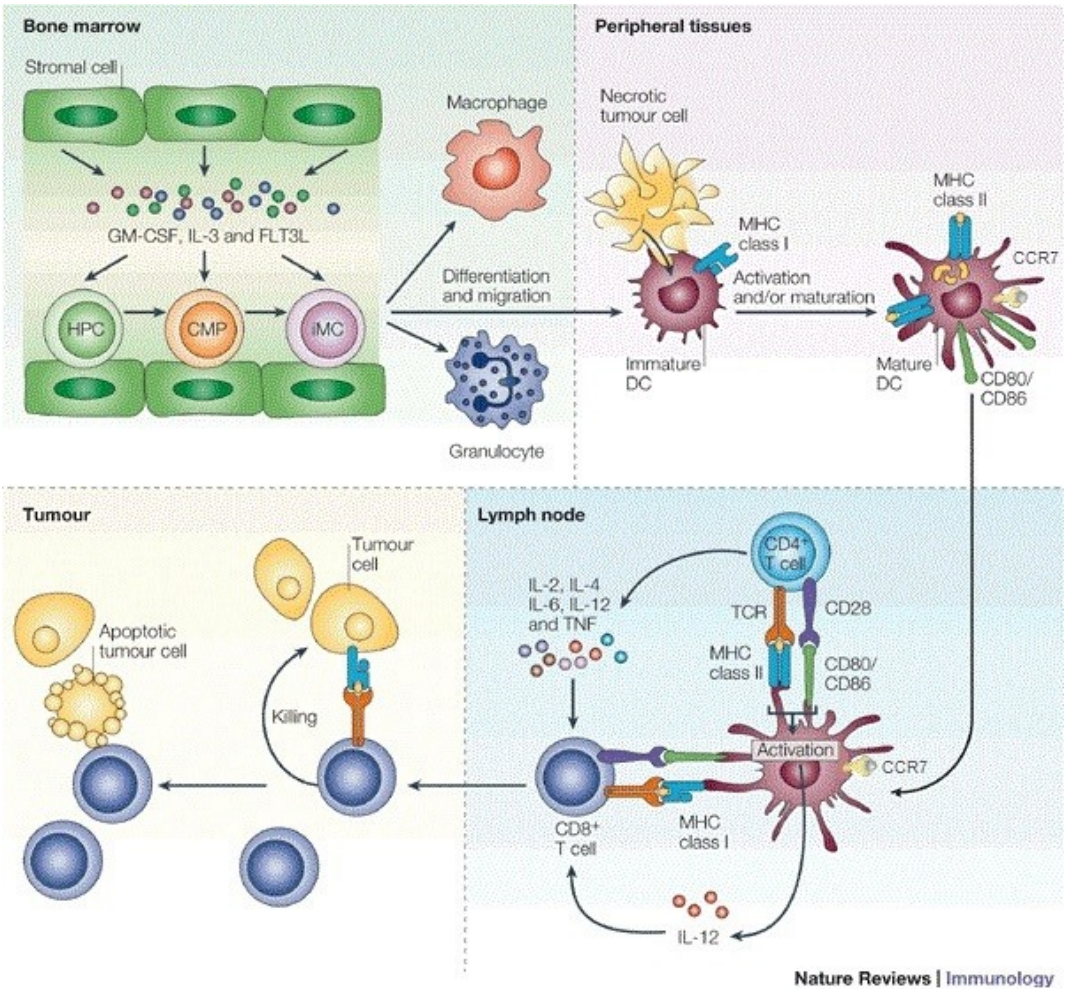

Figure 1.1.5: Modified from "Outline of normal DC differentiation and the role of DC in antitumour immunity" (20)

DC originate from hematopoietic progenitor cells (HPC) cells in the bone marrow, enter the bloodstream (with the intermediate form between the two being the common myeloid progenitor – CMP – which can differentiate into all of the non-lymphoid blood cells) as immature myeloid cells (iMC), then differentiate and migrate towards peripheral tissues where they monitor the environment for antigens (in this example tumour antigen) as iDC. Upon antigen uptake the process of maturation begins. Migratory capacity increases (exemplified by CCR7) and the DC start degrading and presenting the antigen via MHC during migration towards the draining lymph node. They lose their high potential for antigen recognition and endocytosis while profoundly improving their aptitude for antigen-presentation and co-stimulation. In the lymph node, once a suitable T cell makes contact with the MHC presented antigen via its TCR (signal 1), the mDC can supply the necessary costimulatory surface molecules CD80 and CD86 (signal 2) as well as supporting cytokines (e. g. IL-12). Because of their ability to cross-present they can activate both $CD4^+$ and $CD8^+$ T cells. The $CD4^+$ T cells can then provide additional cytokines to help specific $CD8^+$ clonal expansion (or facilitate humoral immunity via T_{h2} differentiation). The $CD8^+$ effector cells then go on to eliminating the structure they have been primed against (tumour cells in this example). TCR – T-cell receptor; TNF – tumour-necrosis factor

1.1.6 Carcinogenesis

Tumour cells have disassociated their growth and proliferation from the external stimuli that tightly regulate normal cell cycles. Internal apoptotic stimuli like DNA damage and the p53 tumour suppressor gene are rendered ineffective, proliferation factors are amplified. Angiogenesis (in solid tumours) is promoted and restrictions on the number of mitotic cycles are lifted.

The aforementioned features are found in cancer as well as benign tumours to some extent; a feature largely exclusive to malignant neoplasms is tissue invasion and metastasis. All of these attributes have been characterized by Hanahan and Weinberg in 2000 (21). They revisited their article in 2011 and added four new characteristics to the previously mentioned six: an unstable genome with resulting mutation, a metabolism which is skewed to favour glycolysis over mitochondria dependent energy generation, tumour-promoting inflammatory processes mediated by invading cells of the immune system and immune escape (22). Immune escape is the ability of tumour cells to evade immune surveillance. It is comprised of several distinct interactions between tumour cells and certain branches of the immune system. Recruitment of T_{reg} cells towards tumour sites, modulation of myeloid cells, down-regulation of tumour antigen expression via MHC I and the ability to induce T cell anergy via TCR binding without co-stimulation contribute to this as well as secretion of cytokines like IL-10 and TGF-β (23).

The iDC subjected to increased levels of these cytokines cannot develop the co-stimulatory capacity of mDC which results in tumour-specific immune tolerance (20). The T_h cell formation is also skewed towards T_{h2} by these cytokines which decreases the efficacy of a CTL response (24).

1.1.7 Cancer Immunotherapy and DC Vaccination

In recent years there have been different approaches to manipulate the immune system into acting against cancer cells: monoclonal antibodies (e.g. trastuzumab for breast cancer treatment) have become a staple in oncology; cytokines like interferons and IL-2 are also used in certain protocols.

Because of their ability to prime naive T cells to a specific antigen, DC are targeted by available vaccines against microbial antigens. They can also be used to vaccinate cancer patients against their tumour. A major advantage of this is that it is a systemic therapy with few side effects which is important because many of the mostly old patients are in poor general health, making them unable to endure harsh chemotherapy regimens. Other advantages over conventional chemotherapy are being independent of the tumour cell cycle (especially in slow-growing tumours) and the possible usage against tumours or metastases of privileged organs like the brain where only few chemotherapy drugs can reach. In these therapeutic vaccinations, the induction of tumour-specific T cells is critically important for their efficacy and is therefore the main goal of tumour vaccines (see figure 1.1.7 a).

There are several ways to develop and administer tumour vaccines, but DC involvement is vital (25).

Vaccine formulations can be based on peptides, proteins, DNA, mRNA, bacteria or viruses, heat shock proteins, antibodies and tumour cells. In the past a multitude of cancer vaccines have been tested, but despite achieving long-lasting remissions in some patients most of them did not meet expectations in terms of clinical response, as published by Filipazzi *et al.* and Leffers *et al.* for peptide-based vaccines in melanoma and ovarian cancer patients, respectively (26, 27). However, some success has been achieved treating metastatic renal cell carcinoma with a combination of a multipeptide vaccine, GM-CSF and the immunosuppressant cyclophosphamide. GM-CSF served as a DC immunostimulant while a cyclophosphamide single-dose 3 days prior to vaccination reduced the number and activity of T_{reg} cells (28). As of now, it is unclear why some vaccines are effective as opposed to others.

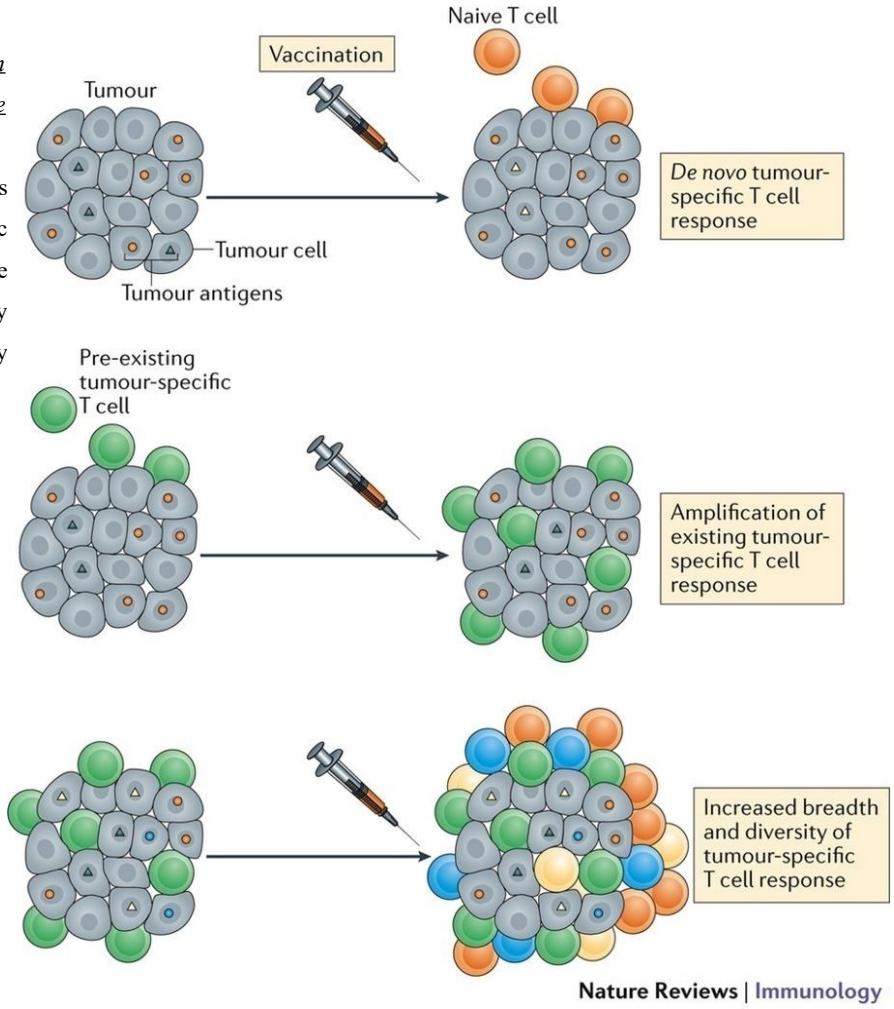

Figure 1.1.7 a: Modified from "Manipulating the immune response to tumours." (29)
The goal of tumour vaccines is to induce a tumor-specific T cell response where none existed before and to amplify or diversify an already existing one.

Being able to create individualized vaccines is an advantageous property of this therapeutic approach. This was already tried on patients with minimal disease lymphoma or in remission after chemotherapy by Kwak *et al.* in 1992 and they succeeded in eliciting an immune response to the vaccine in patients (30). Patient-specific antigens were tested in a vaccine in combination with GM-CSF on follicular lymphoma patients which led to a significant clinical benefit (31). Finding suitable tumour antigens for vaccination is important. Tumour-associated antigens (TAA) and tumour-specific antigens (TSA) are the usually the main subgroups classified. TAA can be regularly occurring antigens which are simply up-regulated on tumour cells (e. g. HER2 and PSA) and TSA can be viral gene products (e. g. stemming from the human papilloma virus) or products of mutated genes (neoantigens) (29).

Neoantigens are especially interesting because some of the corresponding T cell responses have been shown to be associated with tumor regression or long-term disease stability (32, 33).

Adjuvants are important additional components many vaccines. They augment and potentially modify the immunological effect of vaccines. Immune reactions to peptides are mostly very limited so adding at least one adjuvant is imperative for their efficacy as a vaccine. Empirically derived adjuvants and natural or synthetic ligands of different TLR subtypes can be considered for this purpose (34, 35).

Ex vivo generated DC can also be used in therapeutic cancer vaccines. They can be generated either by exposing $CD34^+$ progenitor cells to GM-CSF and FLT3 ligand or monocytes with GM-CSF and IL-4. They are then subjected to the desired antigen after which they may be activated with TNF or TNF and CD40L (see figure 1.1.7 b).

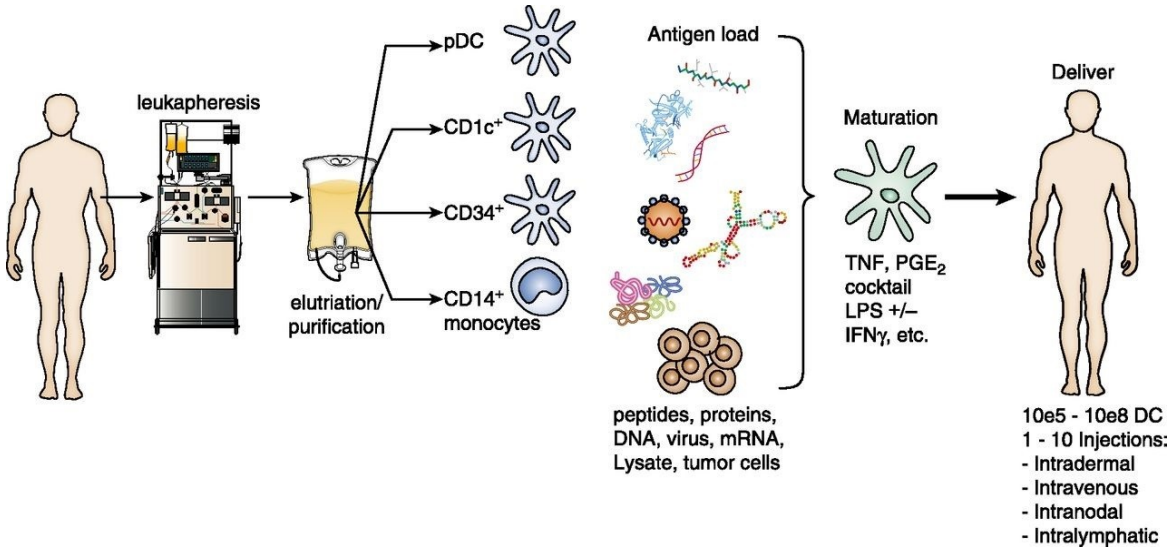

Figure 1.1.7 b: Modified from "The state of the art in translating DC vaccines to the clinic" (36)

This figure shows how a DC vaccine is generated: Patient white blood cells are extracted via leukapheresis and the desired cell type is subsequently separated from the rest and cultivated with suitable cytokines for differentiation into iDC. These cells can then be loaded with different types of antigen as shown. The DC are then provided with a maturation stimulus and prepared for introduction into the patient's system.

These DC have been tested with some success on multiple myeloma patients (37, 38), especially when introduced after an autologous stem cell transplant (39, 40), as well as stage IV melanoma patients (41). Furthermore, a vaccination protocol with this type of

DC has been established and approved by the FDA metastatic castration-resistant prostate cancer after a successful phase 3 trial showed that it prolonged overall patient survival (42). Immune tolerance can also be induced by specific targeting. This has been shown *in vitro* for human DC and *in vivo* for non-human primates (43).

1.2 Multiple Myeloma

Multiple myeloma belongs to the group of non-Hodgkin-lymphoma, more accurately to the subgroup of mature B cell lymphoma. The malignant cell is a plasma cell clone, which often produces abnormal antibodies called paraproteins. These can belong to every immunoglobulin (Ig) subclass. IgG and IgA are the most common, while IgD and IgE types are rare. Another subclass is the light chain myeloma in which the plasma cell clone secretes κ- or λ light chain parts instead of complete antibodies. The most relevant specific risk factor for multiple myeloma is the monoclonal gammopathy of undetermined significance (MGUS), which is defined by the amount of circulating paraprotein, the amount of plasma cells in the bone marrow and the lack of myeloma symptoms in terms of damage or unregulated B lymphocyte proliferation. The prevalence of MGUS is fairly high in the elderly, and while most of them never transform, a large majority of patients have had MGUS prior to multiple myeloma (44). The risk of transformation increases by 1-2 % per year, but since it is primarily a disease of old age, many of the people with MGUS die of some other cause before progressing. Multiple myeloma is distinguished from MGUS by 3 main criteria: more than 10 % bone marrow plasma cells, monoclonal immunoglobulin in serum protein electrophoresis or urine (Bence Jones protein) and myeloma associated organ damage (elevated blood calcium, renal failure, anemia, compromised bone stability).

A patient's prognosis used to be evaluated with the Durie and Salmon staging criteria which were an attempt at objectifying the associated organ damage. The current approach with the Revised International Staging System (R-ISS) only takes into account β2-microglobulin (tumour marker), albumin, cytogenetic risk group and LDH (45). Multiple myeloma cases amount to almost 20 % of hematological and 1.6 % of all

cancers (46); the age adjusted incidence is 6.6/100,000 based on United States data from 2010 to 2014 (47). There are many chemotherapy regimens for inducing and maintaining remission of multiple myeloma. Patients who are physically strong can receive high-dose chemotherapy with subsequent autologous stem cell transplantation. This does not cure the disease but allows for more chemotherapy to be administered and can thus prolong remission and survival (48). Advancements in terms of immunomodulatory drugs including thalidomide, lenalidomide and especially proteasome inhibitors have improved therapeutic options considerably (see chapter 1.2.1), but multiple myeloma still remains mostly incurable with 5-year survival rates of less than 50 % (47). In addition to that, other age-related diseases prevent eligibility for stem cell treatment. Therefore, new treatment approaches are desirable. Avenues that have been explored include specific antibody-chemotherapy conjugates, specific immunomodulatory antibodies, proteasome inhibitors and also anti-tumour vaccines (37, 38, 49).

1.2.1 Proteasome Inhibition as a Therapeutic Principle

In 2008 the FDA granted bortezomib their approval for the initial treatment of multiple myeloma in the USA because its addition to the standard treatment prolonged median patient survival by 5 months in comparison to the standard of melphalan and prednisone (50). Bortezomib inhibits the 26S proteasome with its boron atom (51). The anti-tumour effect of proteasome inhibition suggests that multiple myeloma cells and some other tumours rely on proper proteasome function. The most common side effects are peripheral neuropathy and neuralgia, thrombocytopenia, asthenic conditions, diarrhea, constipation, immunosuppression and anemia. Subcutaneous instead of intravenous administration seems to reduce the occurrence of side effects, especially peripheral neuropathy (52). Clinical response rates are high and can be further improved when combined with dexamethasone in untreated myeloma (53). The response rate in relapsed myeloma is also quite high in combination with cyclophosphamide and dexamethasone (54).

In 2012 the United States FDA granted carfilzomib (trade name: Kyprolis®) their approval for the treatment of relapsed multiple myeloma after failed treatment with bortezomib and immunomodulatory drugs (55, 56). This second-generation proteasome inhibitor is derived from epoxomicin, which is a naturally occuring proteasome inhibitor isolated from an Actinomycetes strain.. Instead of inhibiting the proteasome competitively like bortezomib, it inhibits the 20S proteasome by irreversibly binding to it (57), which leads to an accumulation of proteins that are conjugated with ubiquitin and thus marked for degradation (58). Adverse side effects include thromobcytopenia, anemia, cardiac toxicity, renal impairment, dyspnea, hepatotoxicity and peripheral neuropathy. Cardiac toxicity seems to be more common under carfilzomib treatment when compared to bortezomib while bortezomib causes peripheral neuropathy more often (59).

The ensuing ASPIRE and ENDEAVOR studies have shown high response rates and improved progression free survival in combination with lenalidomide and dexamethasone when compared to the control without carfilzomib for relapsed myeloma (60) and have shown comparable results with only dexamethasone when compared to bortezomib with dexamethasone in relapsed or refractory myeloma (61).

1.3 Effects of Proteasome Inhibition on DC – Project Objective

Disregarding allogeneic stem cell transplantation because of high mortality rates (62), multiple myeloma remains mostly incurable. In a practical sense, however, a long lasting disease remission with low treatment-related side effects can be a worthwhile substitute for a cure. DC based vaccination combined with well tolerated anti-myeloma substances like carfilzomib could be a possible model for this treatment approach. There are at the very least two prerequisites that are paramount for this to be viable: 1. Proteasome inhibition can modulate MHC I dependent antigen presentation (63). If this effect nullified the expression of suitable antigens for targeting on myeloma cells, the success of the aforementioned combined approach would be unlikely. 2. DC have to retain proper function during a treatment regimen that includes carfilzomib.

Previous studies of our working group have shown that bortezomib adversely affects MoDC viability and function in several ways including skewed phenotypic maturation, less migratory and stimulatory capacity, as well as less secretion of inflammatory cytokines and less endocytic capacity (64, 65). Due to its adverse effects on the function of MoDC, bortezomib does not seem to be a suitable candidate for a combined approach with vaccination therapy. As carfilzomib inhibits the proteasome via a different mechanism than its predecessor bortezomib, the effect might be different, less pronounced or even non-existent, which would be most desirable in combination with vaccines. It has been demonstrated that myeloma cells have the ability to evade $CD8^+$ T cells by interacting with the immune system and subsequently down-regulating surface antigens (66). That is why the recent identification of potential targets for vaccination by Walz *et al.* was important. They found 58 highly specific peptides in myeloma cell lines which seemed to elicit a pertinent $CD8^+$ T cell response in myeloma patients (67). Shortly thereafter, Kowalewski *et al.* showed that some of those specific peptides on the MM.1S and the U266 cell lines were stably expressed or even temporarily up-regulated under carfilzomib treatment (68). Sufficient immunogenicity provided, vaccines based on these peptides could improve patient outcome.

In this study we aimed to demonstrate the effect of carfilzomib on human MoDC function compared to the effect of bortezomib in order to assess its suitability for a two-pronged approach with DC vaccination therapy.

2. Materials

2.1 Devices

Table 2.1: Devices

Device	**Manufacturer**
Flow cytometer: FACSCalibur	BD Biosciences, Heidelberg, Germany
Optical microscope: Axiovert 25 CFL	Carl Zeiss AG, Oberkochen, Germany
Sunrise Absorbance Microplate Reader	Tecan Trading AG, Männedorf Switzerland
Pipetboy	INTEGRA Biosciences GmbH, Biebertal, Germany
APT.line C150 (E2) CO_2 Incubator	BINDER, Tuttlingen GmbH, Germany
Laminar flow cabinet	Heraeus Instruments, Hanau, Germany Kendro Laboratory Products, Langenselbold, Germany
Laboratory vacuum pump: VACUSAFE comfort	INTEGRA Biosciences AG, Zizers, Switzerland
Reagenzglasschüttler TYP Reax I	Heidolph Instruments, Schwabach, Germany
MS2 Minishaker	IKA Works, Wilmington, NC, USA
Shaking water bath: No 1083	GFL Gesellschaft für Labortechnik GmbH, Burgwedel, Germany
Freezer -80 °C, Model 8963	Thermo Fisher Scientific, Waltham, MA, USA
Freezer -80 °C, Ultra Low Temperature Freezer UF V 500	BINDER, Tuttlingen GmbH, Germany
Dynatech MR7000 ELISA plate reader	Dynatech Laboratories, Chantilly, USA
Freezer -20 °C	Liebherr, Biberach and der Riss, Germany
Refrigerator 4 °C	Liebherr, Biberach and der Riss, Germany

Mr. Frosty freezing container	Thermo Fisher Scientific, Waltham, MA, USA
Pipettes 10 µl, 100 µl, 200 µl, 1000 µl, Handystep repetitive pipette	Eppendorf, Hamburg, Germany Brand, Wertheim, Germany
Centrifuges	
Thermo IEC Centra-GP8R	ThermoQuest, Engelsbach, Germany
Centrifuge 5804 R	Eppendorf AG, Hamburg, Germany
Heraeus Fresco 17 Centrifuge	Thermo Fisher Scientific, Waltham, MA, USA
Biofuge fresco	Kendro Laboratory Products, Osterode, Germany
Megafuge 1.0 R	Kendro Laboratory Products, Osterode, Germany

2.2 Expendable Materials

Table 2.2: Expendable Materials

Product	**Manufacturer**
SurPhob SafeSeal LOW BINDING filtered tips sterile 10 µl, 100 µl, 1000 µl	Biozym Scientific, Hessisch Olendorf, Germany
Combitips plus 2.5 ml	Eppendorf AG, Hamburg, Germany
Multitips 5 ml	Ritter medical, Schwabmünchen, Germany
Pasteur pipettes, sterile	Roth, Karlsruhe, Germany
5 ml polystyrene round-bottom tube	BD Biosciences, Heidelberg
Eppendorf Safe-Lock Tubes, 1.5 ml	Eppendorf AG, Hamburg, Germany
Tissue culture flask 25 cm^2, 75 cm^2	Corning Falcon, Corning, NY, USA
Conical Centrifuge Tubes, 50 ml	Corning Falcon, Corning, NY, USA
Conical Centrifuge Tubes, 15 ml	Merck KGaA, Darmstadt, Germany

Nunc CryoTubes, conical bottom, starfoot, free standing, 1,0 ml, 1,8 ml	Merck KGaA, Darmstadt, Germany
Falcon Tissue culture plate, 6 well, flat bottom	Becton Dickinson and Co., Franklin Lakes, NJ, USA
Cellstar Cell culture plate, 96 well, flat bottom, U-bottom	Merck KGaA, Darmstadt, Germany
Falcon Cell Culture Inserts, 6.4 mm, 8.0 µm pores	Corning Falcon, Corning, NY, USA
Falcon Tissue culture plate, 24 well, flat bottom	Corning Falcon, Corning, NY, USA

2.3 Agents

2.3.1 Buffers, Solutions, Chemicals

Table 2.3.1: Buffers, Solutions, Chemicals

Product	**Manufacturer**
Dulbecco's Phosphate Buffered Saline, Without CaCl2 and MgCl2 (PBS) 500 ml	SIGMA-ALDRICH, St. Louis, MO, USA
MACS BSA stock solution	Miltenyibiotec, Bergisch Gladbach, Germany
FACS buffer	PBS+25 ml MACS BSA stock solution
Biocoll separating solution	Biochrom AG, Berlin, Germany
Trypan blue	Thermo Fisher Scientific, Waltham, MA, USA
Formalin solution neutral buffered 10 %	SIGMA-ALDRICH, St. Louis, MO, USA
Staurosporine	R&D Systems, Wiesbaden, Germany
Carfilzomib	SelleckChem, Munich, Germany
Kyprolis® (carfilzomib)	Amgen Europe GmbH, Zug, Switzerland
Velcade® (bortezomib)	Millennium Pharmaceuticals (Takeda), Cambridge, MA, USA

2.3.2 Media and Additives

Table 2.3.2: Media and Additives

Product	**Manufacturer**
Gibco RPMI 1640 Medium	Thermo Fisher Scientific, Waltham, MA, USA
X-vivo 20	Lonza, Basel, Switzerland
Fetal calf serum (FCS)	Merck KGaA, Darmstadt, Germany
FcR Blocking Reagent	Miltenyibiotec, Bergisch Gladbach, Germany
Freezing medium	FCS + 10 % DMSO
Antibiotics: penicillin/streptomycin	Thermo Fisher Scientific, Waltham, MA, USA

2.3.3 Fluorescent Antibodies for Flow Cytometry

Table 2.3.3: Fluorescent Antibodies for Flow Cytometry

Product	**Manufacturer**
FITC Mouse IgG1	BD Biociences, San Jose, CA, USA
FITC Mouse Anti Human CD1a	BD Biociences, San Jose, CA, USA
FITC Anti Human CD80	eBioscience, San Diego, CA, USA
FITC Mouse Anti-Human CD209	BD Biociences, San Jose, CA, USA
PE Mouse IgG 1 x Iso Control	eBioscience, San Diego, CA, USA
PE Anti-Human CD83	eBioscience, San Diego, CA, USA
PE Anti-hCCR7	R&D Systems, Minneapolis, MN, USA
Human Osteoactivin Antibody (conjugated with PE in-house)	R&D Systems, Minneapolis, MN, USA
PE Anti-hDC-SIGN	R&D Systems, Minneapolis, MN, USA
PerCP IgG 2B Isotype Control	R&D Systems, Minneapolis, MN, USA
PerCP Anti-CD14	BD Biociences, San Jose, CA, USA
PerCP Anti-hDC-SIGN	R&D Systems, Minneapolis, MN, USA

APC IgG Isotype Control	R&D Systems, Minneapolis, MN, USA
APC Anti-Human HLA-DR	eBioscience, San Diego, CA, USA
APC Mouse Anti-Human CD86	BD Biociences, San Jose, CA, USA
APC Mouse Anti-Human CD209	BD Biociences, San Jose, CA, USA

2.3.4 Cytokines

Table 2.3.4: Cytokines

Product	**Manufacturer**
Leukine (Sargramostim/GM-CSF)	Sanofi-Aventis, Bridgewater, NJ, USA
IL-4	R&D Systems, Wiesbaden, Germany
IL-10	R&D Systems, Wiesbaden, Germany
CCL19/MIP-3β	R&D Systems, Wiesbaden, Germany

2.4 Miscellaneous

Table 2.4: Miscellaneous

Product	**Manufacturer**
ELISA kit: MIP-1α/CCL3	R&D Systems, Wiesbaden, Germany
ELISA kit: RANTES/CCL5	R&D Systems, Wiesbaden, Germany
ELISA kit: IL-6	BD Biociences, San Jose, CA, USA
ELISA kit: IL-12	BD Biociences, San Jose, CA, USA
ELISA kit: MCP-1/CCL2	R&D Systems, Wiesbaden, Germany
Annexin-V-Fluos Staining Kit	Roche Diagnostics GmbH, Mannheim, Germany
Myeloma cell line: U266	Leibniz Institute DSMZ - German Collection of Microorganisms and Cell Cultures GmbH, Braunschweig, Germany
Statistics Software SAS JMP 13 Windows	SAS Institute Inc., Cary, NC, USA

3. Methods

3.1 Generation of Human MoDC

Processing the primary material (buffy coats) to attain MoDC monocultures which are pure enough to use them in subsequent tests takes approximately one week. In the following paragraphs this process will be described in further detail.

3.1.1 Isolating Peripheral Blood Mononuclear Cells

Completely anonymised buffy coats[1] were obtained from blood donations to the blood bank Tübingen for isolating peripheral blood mononuclear cells (PBMC). It was done by diluting the buffy coat at a 1:4 ratio with phosphate buffered saline (PBS) and then layering it over a cell separating solution (Biocoll seperating solution). This polymer solution has a molecular weight of 400,000 Dalton and a density of 1.077 g/ml. 30 ml of diluted buffy coat were layered over 12 ml of cell separating solution. After 20 minutes of centrifugation at 806·g and room temperature, there were four visible layers in order from top to bottom of the tube: plasma layer, layer of mononuclear cells and thrombocytes, separating solution, layer of non-mononuclear cells. The layer of the mononuclear cells was then removed with a pasteur pipette and transferred to 2 unused tubes.

To remove any remnants of the separating solution, these cells were then rinsed twice by adding approximately 45 ml of PBS and removing the supernatant after 5 minutes in the centrifuge at 453·g. To remove a portion of the thrombocytes, the cells were then rinsed a third time at 250·g after adding 25 ml of PBS. The cells were then combined in one tube and counted. After another 5 minutes in the centrifuge, the cells were dispersed in X-Vivo 20 cell medium and distributed evenly across several cell culture flasks for adhesion of the peripheral blood monocytes (69).

1 The use of anonymised buffy coats has been approved by the ethics board of the University. No personal data of any donor was received or used in this study.

3.1.2 Counting Live PBMC in the Neubauer Chamber

The PBMC pellet was dispersed in 40 ml of PBS. 10 µl of the cell suspension, and 10 µl of Trypan blue were diluted with 80 µl of PBS, so a 1:10 dilution was achieved. 10 µl of blue dyed diluted cell suspension were then transferred into the Neubauer chamber. Cells were counted in diagonally opposite fields of 16 squares each. The cell count in 40 ml of cell suspension was calculated as follows:

$$Cellcount \cdot 0.5 \cdot 40 \cdot 10 \cdot 10^4$$

The factor 0.5 is used for creating the mean count from both fields counted, 40 is the total volume of cell suspension in ml, 10 is the dilution factor of the cell suspension in the Neubauer chamber relative to the 40 ml of cell suspension and 10^4 is the constant factor of the Neubauer chamber.

3.1.3 Starting MoDC Cultures

MoDC cultures were started using 75 cm^2 cell culture flasks with no more than $12 \cdot 10^7$ and no less than $6 \cdot 10^7$ peripheral blood mononuclear cells (PBMC) in 10 ml of cell culture fluid. Cell cultures with low yields of PBMC were started using 25cm^2 cell culture flasks with no more than $5 \cdot 10^7$ and no less than $3 \cdot 10^7$ PBMC in 5 ml of cell culture fluid.

After no less than 90 minutes and no more than 120 minutes of adhesion time at 37 °C and 5 % CO_2, the non-adherent cells were rinsed off with the X-Vivo 20 in their respective flask and room temperature PBS; the X-Vivo 20 was replaced by RPMI cell culture medium with bovine fetal calf serum and penicillin/streptomycin as additives (69). IL-4 (20 ng/ml cell suspension) and GM-CSF (100 ng/ml cell suspension) were added to each cell culture flask immediately and every other day for inducing the differentiation of monocytes into MoDC (69, 70). DMSO was added to the negative control and IL-10 (10 ng/ml cell suspension) was added to the positive control for

altering (stunting) that differentiation (71, 72). Bortezomib was also added to one of the flasks for comparison (see Table 3.1.4). The cells were incubated for 7 days at 37 °C and 5 % CO_2.

3.1.4 Administering Carfilzomib and Bortezomib

On the day before harvesting the MoDC were subjected to varying doses of carfilzomib in DMSO solution and its medical grade equivalent in 5 % glucose solution. The doses were administered by using new cell culture medium enriched with IL-4 and GM-CSF and adding the desired dose. The cells were separated from their medium via centrifuge. The medium was preserved so the cells could be re-suspended in their previous microenvironment after having been subjected to carfilzomib. The MoDC were then suspended in the carfilzomib medium and incubated at 37 °C and 5 % CO_2 for 60 minutes. After incubation they were taken out of the flasks again and separated from the carfilzomib via centrifuge. During centrifugation the flasks were rinsed with 10 ml of RPMI medium which was then added to the cells for another 5 minutes of centrifugation. Afterwards, the cells were re-suspended in the preserved medium. For the carfilzomib concentration and duration of exposure, we oriented ourselves according to previous studies on the IC_{50} concentration in multiple myeloma cell lines and the pharmacokinetics of carfilzomib (58, 73, 74). The Protocol for bortezomib was chosen in accordance with the previous publication (65) by adding the desired dose directly into the flask (see Table 3.1.4). LPS was added to the MoDC that were designated to become mature MoDC (mMoDC) (75) 16 hours before the cell harvest. The cells without LPS were labeled immature MoDC (imMoDC).

Table 3.1.4: Trial Set-up

	1	2	3	4	5
Day 0,2,4,6	IL-4/GM-CSF	IL-4/GM-CSF	IL-4/GM-CSF	IL-4/GM-CSF	IL-4/GM-CSF/IL-10
Day 6	DMSO (+LPS)	100nM carfilzomib (+LPS)	100nM Kyprolis (+LPS)	1ng/ml bortezomib/24 h (+LPS)	(+LPS)
Day 7	Harvest				

3.1.5 Harvesting MoDC

The first step was separating the cells from the culture fluid via centrifugation, preserving some of the culture fluid for immunoassays and re-suspending the cells in PBS. The internal surface of the culture flasks was also rinsed with 10 ml of room temperature PBS to release as many cells as possible from it. This was added to the remaining culture fluid and centrifuged again. The MoDC yield was different each time and the amount of PBS, usually between 2 ml and 5 ml, was chosen according to the cell pellet size. The total MoDC count was then determined with the same method used for determining the PBMC count (see 3.1.2) with the only differences being the concentration of cell suspension (which was 1:2) and the varying amount of PBS (fixed at 40 ml for the PBMC count) :

$$Cellcount \cdot 0.5 \cdot Volume_{PBS} \cdot 2 \cdot 10^4$$

The preserved culture fluid (four 1 ml portions) was labeled and frozen at -20 °C.

3.2 Flow Cytometry

Flow cytometry is a technological method which is used to determine size and properties of microscopic particles, e. g. cells. Its analytic potential can be enhanced by labeling the particles with fluorescent markers. An example for the non-enhanced method would be a regular blood count, a blood panel frequently requested by physicians. Fluorescence-activated cell sorting (FACS) is used less frequently in the medical field, e. g. in HIV staging diagnostics for determining the $CD4^+$ T cell count, but plays a significant role in biochemical and medical research because it allows for the assessment of the type and amount of cellular surface molecules expressed in a cell population.

The process of FACS flow cytometry can be described as follows:

A sample of fluorescence labeled cells suspended in a special buffer solution is gradually aspirated into the flow cytometer. The cells then pass through a tube which can only accommodate one cell at a time, so single cells can be analysed. During their transit, the cells are hit with a focused laser beam, and two types of the resulting light scatter are recorded by detectors: The forward scatter (FSC) in line with the laser beam and the side scatter (SSC) perpendicular to the laser beam's path. Depending on the detected scatter, each cell is directed towards a certain container via electrical charge. FSC is largely dependent on cell size, while SSC is determined by granularity, fluorescence, nucleic size and number of vesicles.

3.2.1 Labeling MoDC with Fluorescent Antibodies

To analyse molecular patterns on the surface of MoDC, pertinent molecules have to be labeled with detectable structures. Each of these molecules requires a specific structure for labeling, usually an antibody with a radioactive or fluorescent molecule attached.

To evaluate the phenotype of every MoDC yield, fluorescent antibodies specific to MoDC surface molecules were used, some of which are crucial for proper MoDC function.

Table 3.2.1: FACS Antibodies – Target and Colour

Molecular Target	**Colour**
IgG1	FITC, PE, APC
IgG2b	PerCP
CD1a	FITC
CD80	FITC
CD83	PE
Osteoaktivin	PE
CCR7	PE
CD14	PerCP
DC-SIGN	PerCP, (FITC, PE, APC for single stain compensation)
HLA DR	APC
CD86	APC

After transferring anywhere from $0.5 \cdot 10^6$ to 10^6 cells of each type into flow cytometry tubes, the unspecific binding sites had to be blocked with an FcR blocking agent. After 10 – 20 minutes of dark incubation, these cell amounts were divided into thirds. Each third was then stained with a mixture of 4 antibodies with different fluorescent colours: FITC, PE, PerCP and APC.

Some of these colours have overlapping light spectra, which is why single stains with these colours were necessary for every MoDC phenotype in every trial. These single stained cells were fed into the flow cytometer to adjust its settings just before the actual multi-stain analysis. The difference in median fluorescence intensity (DMFI) between isotype control and a specific molecule served as a stand-in value for the expression of the analysed surface molecule.

For better comparability between trial runs, I calculated the normalized DFMI by dividing the DMFI of the treated cells by the DMFI of the untreated cells for each trial. Example:

$$DMFI_{imMoDC/IL\text{-}10} \,/\, DMFI_{imMoDC/DMSO}$$

3.3 Enzyme-Linked Immunosorbent Assay (ELISA)

An enzyme-linked immunosorbent assay, usually better known as ELISA, is a method by which a specific constituent of a solution can be detected and identified via change in colour or light emission. There are different types of ELISA, but they work in a similar fashion: A specific antibody or antigen attached to a surface binds to the molecule which is supposed to be detected. The surface is subsequently rinsed of the unbound substances, then an enzyme-conjugated antibody is introduced which also binds to the detected and bound constituent. After rinsing off the excess amount of this second antibody, the enzyme receives a suitable substrate to produce colour, fluorescence or light which can then be quantified by measuring the light extinction in comparison to a dilution series of a known standard.

The ELISA assays used in this project were sandwich-ELISA: The surface-attached agent was a so-called capture antibody and the second an enzyme-linked detection antibody. In this kind of ELISA the detection antibody and the capture antibody have to bind to mutually exclusive epitopes to prevent one antibody from interfering with the binding of the other. In the following paragraph the procedure will be explained in detail on the basis of one example.

The plate wells were pre-coated with a capture antibody. After preparing the buffer, substrate solution and cytokine standard according to instructions, the cytokine standard and the buffer were used to create a dilution series through which concentration and optical density could be correlated on the resulting graph.

200 µl of standard, control or sample were added into each plate well, then incubated at room temperature for 2 hours. After washing three times and removing the liquid, 200 µl of detection antibody solution were added into each well. After 1 hour of incubation the washing procedure was repeated and the excess liquid removed. 200 µl of the substrate solution was then added into each well. After 20 minutes of dark incubation at room temperature 50 µl of Stop solution were added into each well. The optical density was analysed with a microplate reader at a 450 nm wavelength within 30 minutes.

The purpose of the ELISA method in the context of determining MoDC function was to

quantify MoDC cytokine production after exposure to carfilzomib.

Table 3.3: Measured Cytokines and Their Functions

Cytokine	**Function**
MIP-1α/CCL3	Inflammation, acute phase-, fever inducing
Rantes/CCL5	Promotes T cell immunity
IL-12	Granulocyte activation, promotes release of IL-1, IL-6, TNF
IL-6	Attracts immune cells to inflammation focus
MCP-1/CCL2	Attracts immune cells to inflammation focus

3.4 Cell Viability

3.4.1 Annexin / Propidium Iodide (PI) staining of MoDC

The annexin-V-fluorescein / PI staining assay can be used for assessing cell viability. Annexin is a compound that binds to phospholipids, especially phosphatidylserine, which exclusively occur on the inner, cytoplasm-facing leaflet of a cell's membrane. It is "flipped" to the outer leaflet during early apoptosis (76). PI is a dye which binds to the DNA. As it cannot pass through intact cell membranes, it only stains cells with a ruptured cell membrane which is a characteristic of both necrosis and late apoptosis (77).

In a 96 flat well plate the cell amount per well was 10^5 MoDC in cell culture medium with 4 wells per MoDC type, one of which was used for unstained and single stain annexin and PI. The unstained and single stain cells were used for adjusting voltages and compensation. The negative control MoDC had to be divided among 3x4 wells because of internal negative and positive control MoDC. The internal positive control for the assay was done by adding staurosporine to each well, the negative control consisted of adding DMSO. The plate was then incubated for 20-24 h at 37 °C and 5 % CO_2. After incubation the cells were harvested and transferred into FACS tubes and centrifuged, the supernatants were discarded. The cells were then re-suspended in the

annexin incubation buffer and stained with either annexin-V-Fluos, PI (for the single-stain) or both (the other cells). After 15 minutes of dark incubation the cells were immediately analysed via flow cytometry. Cells further right on the x axis in the Q3 quadrant (lower right) have taken up more annexin than the unspecific amount in the Q4 (lower left) quadrant. This signifies early apoptosis. Cells also higher up on the y axis inside the Q2 (upper right) quadrant have taken up more PI than the unspecific amount in Q3 and Q4. The percentage given in each quadrant is the fraction of all events recorded in that quadrant. Cells in the Q4 quadrant have only taken up unspecific amounts of annexin and PI, not signifying early or late apoptosis.

3.4.2 Annexin / Propidium Iodide staining of U266 Cells

The annexin / PI stain of the U266 multiple myeloma cells was conducted in the same manner as the MoDC stain (see chapter 3.4.1) but with different cell yields: $5 \cdot 10^5$ per well for 24 well plates and $1.5 \cdot 10^6$ per well for 6 well plates. The U266 cells were subjected to varying concentrations of carfilzomib in its compound- as well as in its medical grade version and bortezomib in accordance with their respective protocols before being processed in this assay.

3.5 Migration towards CCL19/MIP-3β

The migratory capacity of imMoDC and mMoDC was assessed by making them pass a micro-pore cell culture insert.

After the MoDC harvest $6 \cdot 10^5$ cells were re-suspended in RPMI cell culture medium at a concentration of $2 \cdot 10^5$/ml. Each well of a 24 flat well plate was filled with 1 ml of RPMI cell culture medium enriched with CCL19/MIP-3β at a concentration of 100ng/ml. The next step was to place cell culture inserts with 8 µm pores into the plate wells and fill them with 1 ml of the preciously prepared cell suspension – 3 plate wells for each MoDC type. Cell migration along chemotactic gradients also occurs *in vivo*. A well known example for this would be leukocytes leaving the bloodstream through

more permeable blood vessels at an inflammation site.

After 16 hours of incubation at 37 °C and 5 % CO_2, the cell culture inserts were removed and discarded. The fluid in the plate wells was then transferred into FACS tubes. Each plate well was rinsed with its contained fluid once to loosen MoDC adherent to the bottom of the well. The cells were centrifuged for 5 minutes at 1500 rpm and re-suspended in flow cytometry buffer. The amount of cells aspirated during the course of 60 seconds was then measured with the flow cytometer. The cell count is a stand-in value for the migrated cells (not all of the cells are aspirated within 60 seconds).

3.6 Freezing Cells

MoDC can be preserved for later use by freezing them at -80 °C in a freezing medium consisting of FCS with a 10 % volume fraction of DMSO. After counting the MoDC in PBS and subsequent centrifugation, the cells have to be re-suspended in the freezing medium at a cell concentration which is equal to or below 10^7/ml. The transfer into the special freezing tubes as well as the transfer of those tubes into the freezing container and the transport to the -80 °C freezer all have to happen quickly because of DMSO toxicity at warmer temperatures. The freezing container is filled with isopropyl alcohol which cools the cells by -1 °C/min approximately. After having been completely frozen, the cells may be stored in another container.

3.7 Thawing Cells

Before thawing the frozen cells, 20 ml of the right cell culture medium were heated to 37 °C. With a 1000 µl pipette the solid block of frozen cell suspension were dissolved in the warm medium and centrifuged quickly because of the aforementioned DMSO toxicity. After discarding the supernatant, the pellet was re-suspended in another 20 ml of warm medium and centrifuged again. The cells were then be re-suspended in 5-10 ml of medium, counted and sown into the appropriate cell culture container.

3.8 Cultivating the Non-Adherent U266 Multiple Myeloma Cells

After thawing the U266 cells, suspending them in RPMI (+FCS) medium and seeding them out at $0.5 \cdot 10^6$/ml, the cell population was split regularly because the cells consume the medium for their infinite replication cycles. The cell count was determined (also in the Neubauer chamber but suspended in their culture fluid instead of PBS) for the first few splits. After discarding about 2/3 of the cell amount, the cells are then provided with fresh medium. This step has to be repeated within 2 days after the last split for as long as the cell culture is supposed to be maintained. The cells were incubated at 37 °C and 5 % CO_2; their concentration did not exceed 10^6/ml. The medium and the method of sowing the cells were done according to instructions given by the Leibniz Institute DSMZ-German Collection of Microorganisms and Cell Cultures GmbH.

3.9 Statistical analysis

Each experiment was realized at least three times revealing similar results. Representative experiments as well as combined data are shown. If not otherwise declared, technical triplicates were performed leading to an average value and enabling the calculation of a standard error of the mean. To prove statistical significance Dunnett's test was applied if not otherwise declared; p values < 0.05 were considered suggesting statistical significance. Values deviating more than two standard deviations from the mean were considered outliers and excluded from the final analysis. Statistical analysis was performed with SAS JMP 13 for Windows.

4. Results

The objective of this project was on discovering a possible change in the MoDC phenotype due to carfilzomib. MoDC function was tested with regard to cell viability, cytokine secretion and migration. Asterisks signify statistical significance.

4.1 Cell Viability

These trials were conducted to find a dosage that is sufficiently high for myeloma treatment while maintaining a low degree of MoDC toxicity.

4.1.1 Higher Doses of Carfilzomib Induce Apoptosis in MoDC

Proteasome inhibition facilitated by carfilzomib does not selectively target multiple myeloma cells, and therefore an effect on cell viability of normal cells is possible. Analysis in an annexin / propidium-iodide assay for assessment of apoptosis and cell death showed a decrease in MoDC viability after exposure to the 300 nM carfilzomib dosage, especially if the cells were stimulated with LPS thereafter (see figure 4.1.1 a). The trials with 300 nM carfilzomib had to be discontinued because they did not yield the minimal amount of cells required for analysis. The majority of mMoDC treated with 300 nM carfilzomib showed an increase in annexin uptake indicating early apoptosis. The non-stimulated imMoDC also showed an increase in annexin uptake after exposure to the same amount of carfilzomib.

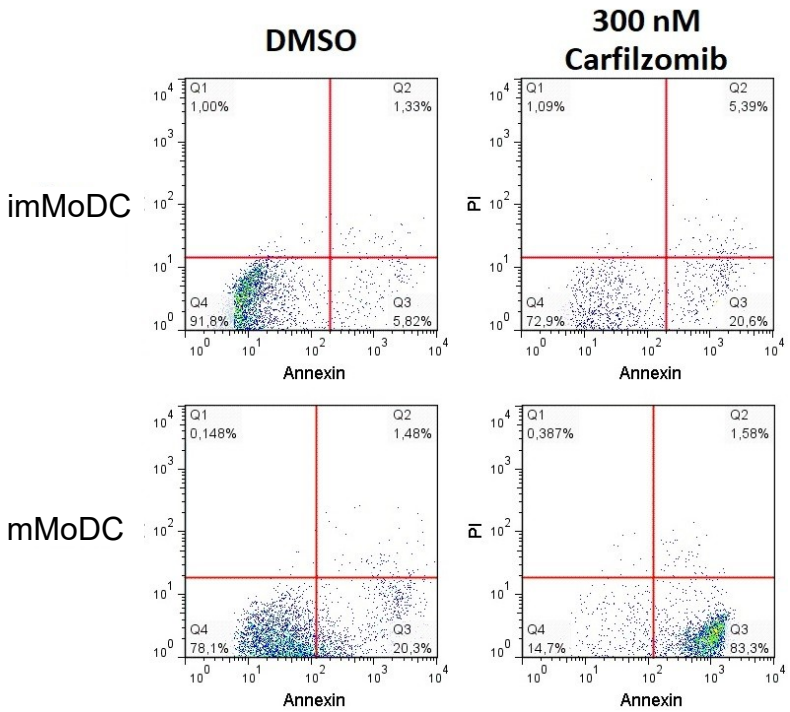

Figure 4.1.1 a: Example of flow cytometry dot plots following an annexin / PI assay with MoDC. Cells further right on the x axis in the Q3-quadrant have taken up more annexin than the unspecific amount in the Q4 quadrant. This signifies early apoptosis. Cells that are also higher up on the y axis and have entered the Q2 quadrant have taken up more PI than the unspecific amount in the Q3 and Q4 quadrants indicating membrane integrity loss (end stage apoptosis). The percentages given in each quadrant is the fraction of all events recorded in that quadrant. N=2

The 100 nM dosage of carfilzomib and Kyprolis appeared to be considerably less toxic with respect to apoptosis and necrosis. The yield of viable cells was much closer to the DMSO control (see figure 4.1.1 b). Compared to the DMSO control, there is only a small increase in annexin or annexin and PI uptake in both imMoDC and mMoDC after exposure to 100 nM carfilzomib or Kyprolis.

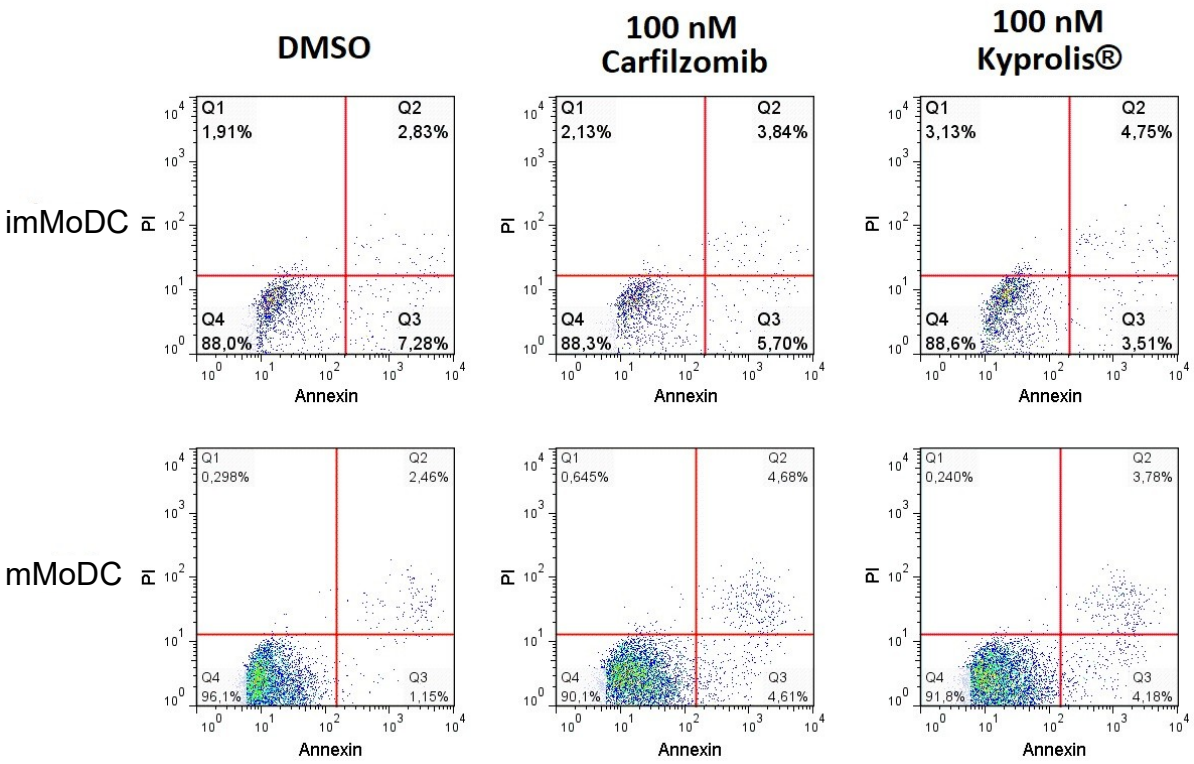

Figure 4.1.1 b: Example of flow cytometry dot plots following an annexin / PI assay with MoDC. Cells further right on the x axis in the Q3-quadrant have taken up more annexin than the unspecific amount in the Q4 quadrant. This signifies early apoptosis. Cells higher up on the y axis in the Q2 quadrant have taken up more than the spontaneous amount of PI in the cells of the Q3 and Q4 quadrants. The percentages given in each quadrant is the fraction of the all events recorded in that quadrant. . N=3

4.1.2 Effect of Carfilzomib Dosage on Viabilty of Myeloma Cell Line U266

To find out how the 100 nM dosage of of carfilzomib and Kyprolis would compare to higher dosages in terms of an anti myeloma effect, we compared dosages up to 1000 nM carfilzomib in an annexin / propidium-iodide assay with cells from a U266 multiple myeloma cell line. The non-medical grade compound was compared with the medical grade compound Kyprolis to compensate for possible impurities or byproducts in the non-medical grade compound as confounding factors. There seemed to be little difference between combined percentages of all apoptotic cells in the cells treated with

100 nM, 300 nM and 1000 nM carfilzomib. Kyprolis seemed to be less potent than the chemical compound. 30 nM carfilzomib appeared to be inferior regarding induction of apoptosis *in vitro*. The 1 ng/ml (2.6 nM) bortezomib dosage seemed to be inferior to 30 nM carfilzomib in this regard. All of these trials were conducted with the same carfilzomib lot. All of the aforementioned results were statistically significant in one-tailed t-tests ($p<0.05$).

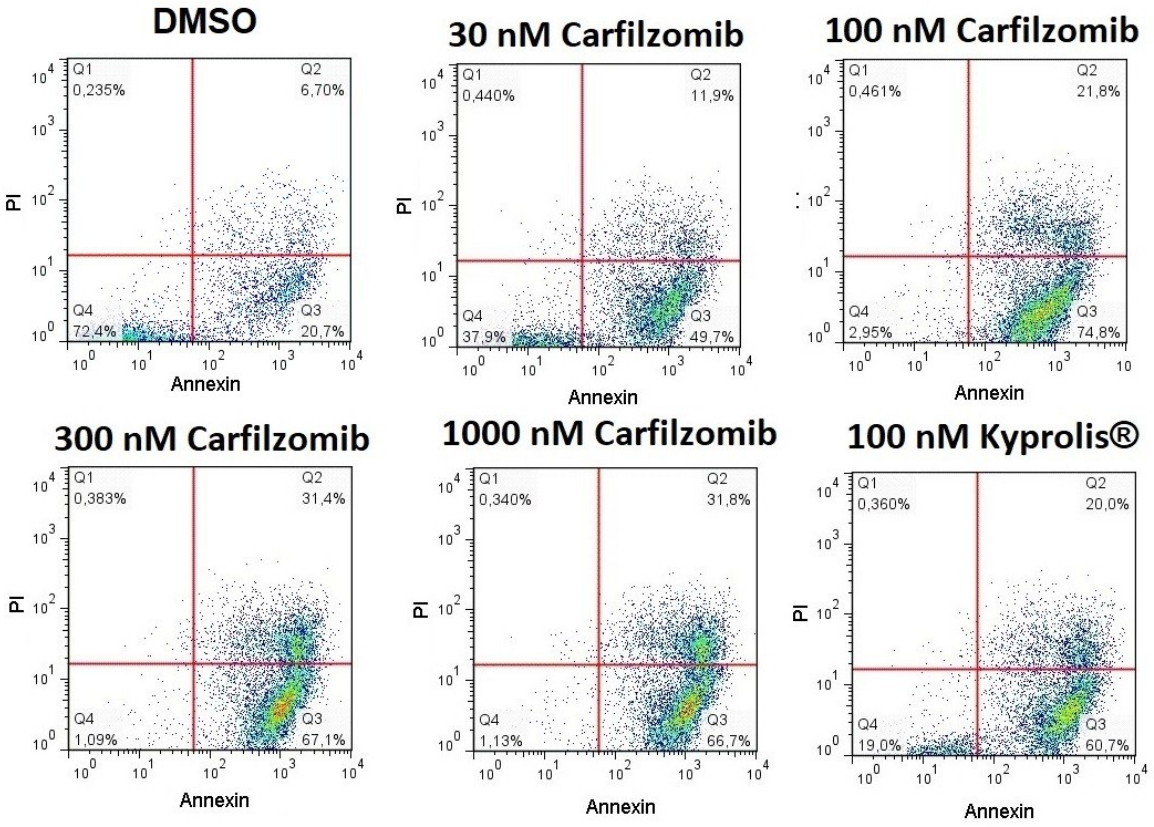

Figure 4.1.2 a: Example of flow cytometry dot plots following an annexin / PI assay with U266 multiple myeloma cells. Cells further right on the x axis in the Q3-quadrant have taken up more annexin than the unspecific amount in the Q4 quadrant. This signifies early apoptosis. Cells also higher up on the y axis inside the Q2 quadrant have taken up more PI than the unspecific amount in Q3 and Q4. The percentage given in each quadrant is the fraction of all events recorded in that quadrant. N=3

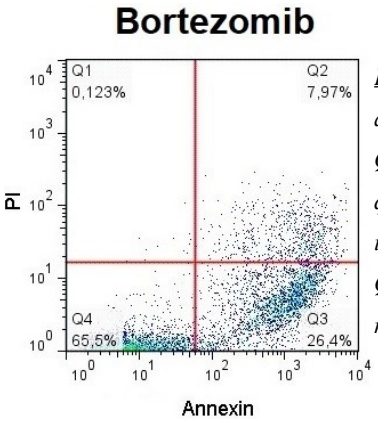

Figure 4.1.2 b: Example of flow cytometry dot plots following an annexin / PI assay with U266 multiple myeloma cells. Cells further right on the x axis in the Q3-quadrant have taken up more annexin than the unspecific amount in the Q4 quadrant. This signifies early apoptosis. Cells also higher up on the y axis inside the Q2 quadrant have taken up more PI than the unspecific amount in Q3 and Q4. The percentage given in each quadrant is the fraction of all events recorded in that quadrant. N=3

100nM carfilzomib was identified to be effective in induction of apoptosis in U266 myeloma cell line cells *in vitro* while limited toxicity in MoDC was observed which is why consecutive experiments were focused on the 100 nM carfilzomib dosage.

4.2 MoDC Phenotype

MoDC were treated with100 nM carfilzomib on day 6 of the cell culture. Possible changes of the MoDC phenotype after exposure on day 6 were detected by FACS analysis on day 7. In the following experiments the effects of 100 nM carfilzomib on the phenotype of MoDC was assesed. A phenotype baseline can be established by compiling overlays of DMSO treated MoDC (see figure 4.2). IL-10 served as a positive control because it hampers differentiation of monocytes into MoDC (78).

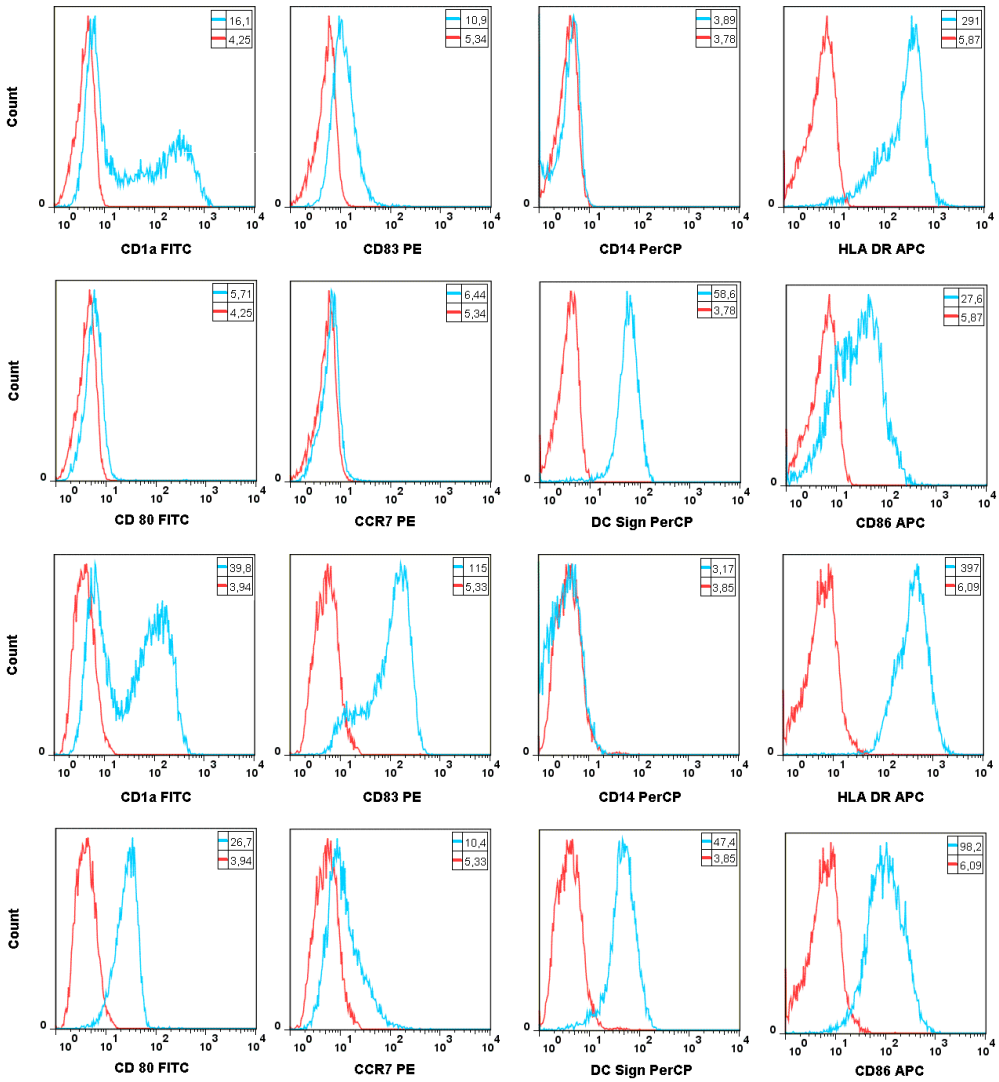

Figure 4.2: Normal Phenotype of Untreated imMoDC and mMoDC. Row 1-2: untreated imMoDC, row 3-4: untreated mMoDC; X-Axis: Surface expression; y axis: cell count; red: IgG-isotype; blue: phenotype

4.2.1 Exposure to Carfilzomib Does Not Affect the Expression of CD14 in MoDC

CD14 is a surface molecule especially found on monocytes. In this line of experiments the loss of CD14 expression signifies the successful differentiation of monocytes into MoDC (see figure 4.2.1 a-c). The cells treated with IL-10 served as positive control, the ones treated with DMSO as negative control. As shown in Figures 4.2.1 a-c, treatment of MoDC with 100 nM carfilzomib had no significant effect on CD14 expression while higher maintained CD14 expression in IL-10 treated cells could be observed ($p<0.05$).

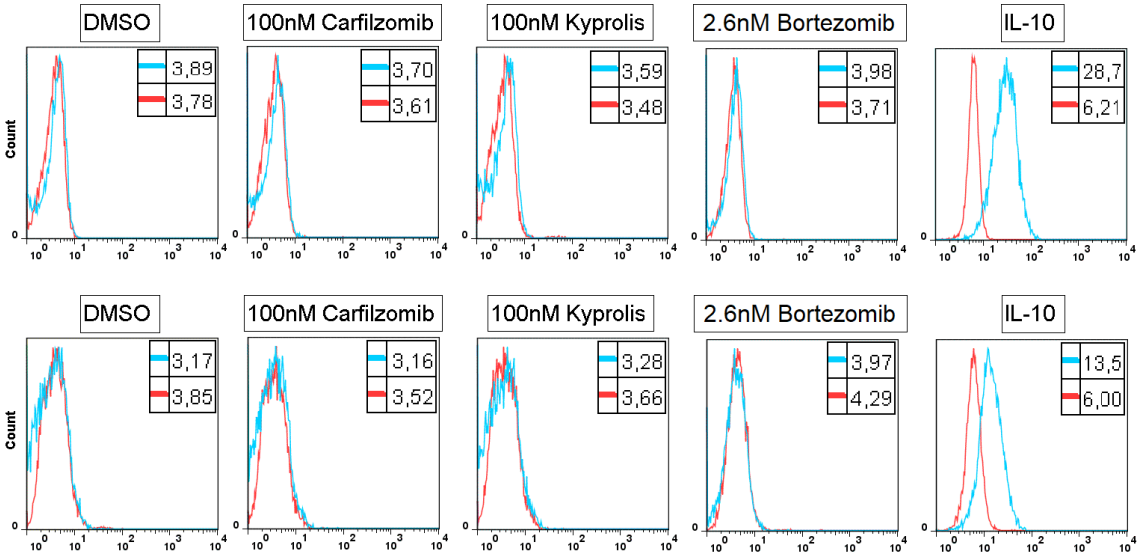

Figure 4.2.1 a: ImMoDC and mMoDC were stained with a fluorescent anti-CD14, then analysed via flow cytometry. The histograms in this example show very low expression of CD14 as would be expected from MoDC. Cells treated with IL10 showed higher CD14 expression. Top row: imMoDC, bottom row: mMoDC; X-Axis: CD14 expression; y axis: cell count; red: IgG-isotype; blue: CD14

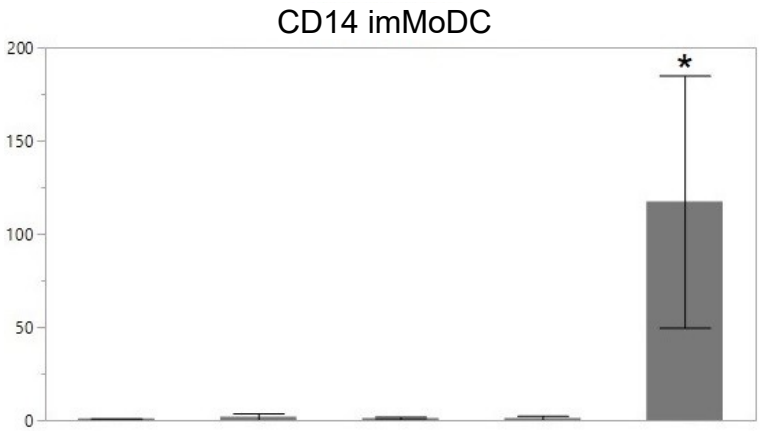

Figure 4.2.1 b: Average and standard deviation of the DMFI in each imMoDC group. The values were normalized to 1.00 for DMSO treated imMoDC. Columns left to right: DMSO, 100 nM carfilzomib, 100 nM Kyprolis, 1 ng/ml=2.6 nM bortezomib/ 24 h, IL-10; y axis: DMFI; asterisks signify statistical significance; N=8

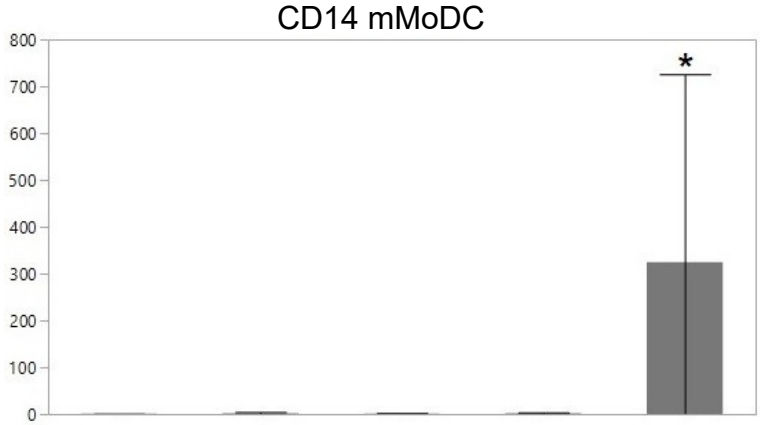

Figure 4.2.1 c: Average and standard deviation of the DMFI in each mMoDC group. The values were normalized to 1.00 for DMSO treated mMoDC. Columns left to right: DMSO, 100 nM carfilzomib, 100 nM Kyprolis, 1 ng/ml=2.6 nM bortezomib/ 24 h, IL-10; y axis: DMFI; asterisks signify statistical significance; N=10

4.2.2 Exposure to Carfilzomib Does Not Affect the Expression of CD1a in Unstimulated or LPS Stimulated MoDC

CD1a is a surface protein, which, like the structurally related MHC proteins, is involved in antigen-presentation. It is also a marker for IL-12 secreting DC (79). Carfilzomib and Kyprolis exposure had no statistically significant effect on the expression of the CD1a molecule in unstimulated or LPS stimulated mMoDC while exposure to bortezomib produced a statistically significant decrease in imMoDC and mMoDC (see figure 4.2.2 a and b; $p<0.05$). For mMoDC, but not for imMoDC, this has been demonstrated in our previous study (65).

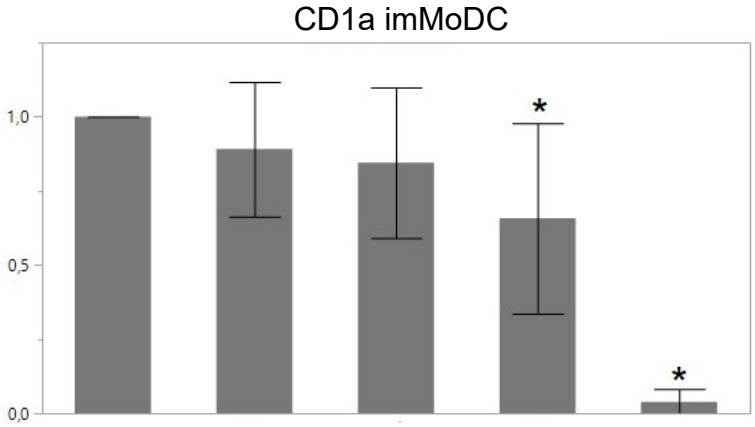

Figure 4.2.2 a: Average and standard deviation of the DMFI in each imMoDC group. The values were normalized to 1.00 for DMSO treated imMoDC. Columns left to right: DMSO, 100 nM carfilzomib, 100 nM Kyprolis, 1 ng/ml=2.6 nM bortezomib/ 24 h, IL-10; y axis: DMFI; asterisks signify statistical significance; N=10

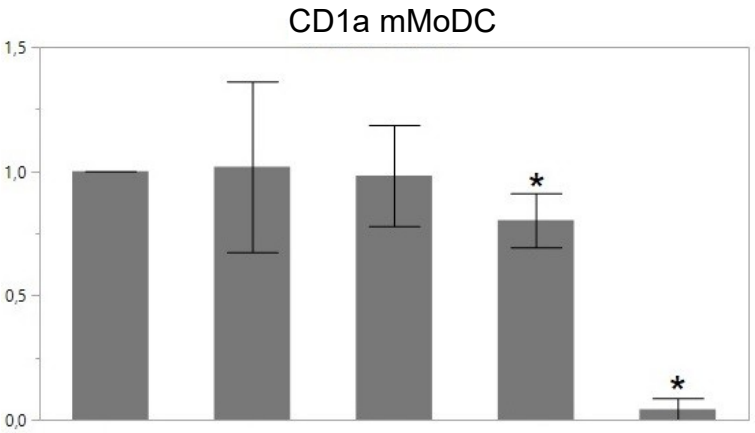

Figure 4.2.2 b: Average and standard deviation of the DMFI in each mMoDC group. The values were normalized to 1.00 for DMSO treated mMoDC. Columns left to right: DMSO, 100 nM carfilzomib, 100 nM Kyprolis, 1 ng/ml=2.6 nM bortezomib/ 24 h, IL-10; y axis: DMFI; asterisks signify statistical significance; N=9

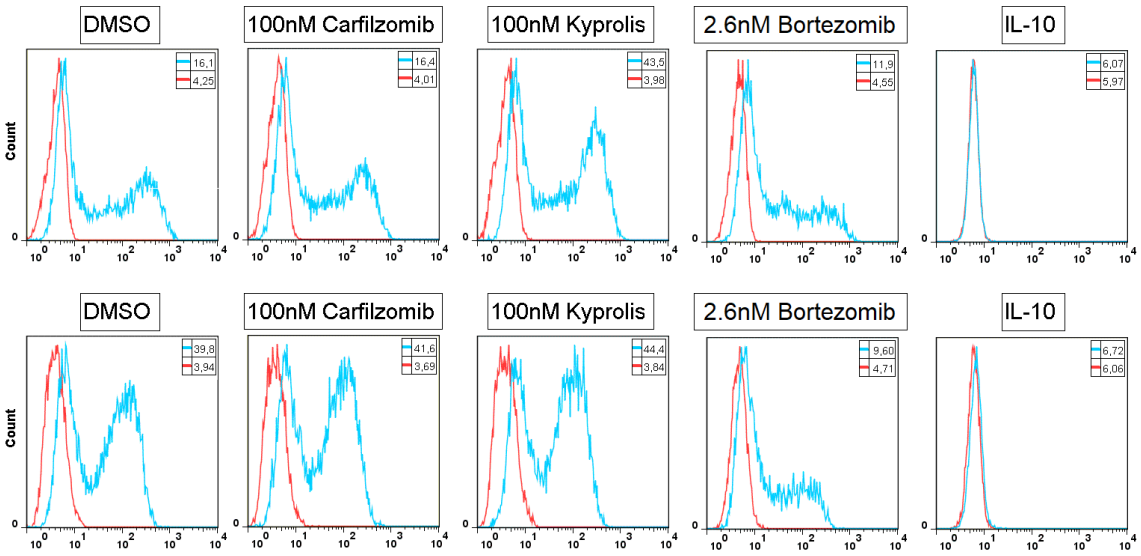

Figure 4.2.2 c: Exemplary overlay of a CD1a trial. Top row: imMoDC; bottom row: mMoDC; y axis: cell count; red: IgG-isotype; blue: CD1a

4.2.3 Exposure to Carfilzomib Does Not Affect the Expression of CD209/DC-SIGN in Unstimulated or LPS Stimulated MoDC

As a C-type lectin receptor, CD209/DC-SIGN recognizes mannose based microbial PAMPs (80). Neither Carfilzomib nor Kyprolis had a statistically significant effect on the expression of DC-SIGN/CD209 in unstimulated or LPS stimulated mMoDC (see figure 4.2.3 a and b; $p>0.05$) while bortezomib exposure produced a statistically significant decrease in LPS stimulated mMoDC (see figure 4.2.3 b; $p<0.05$) which has also been demonstrated in our previous study (65).

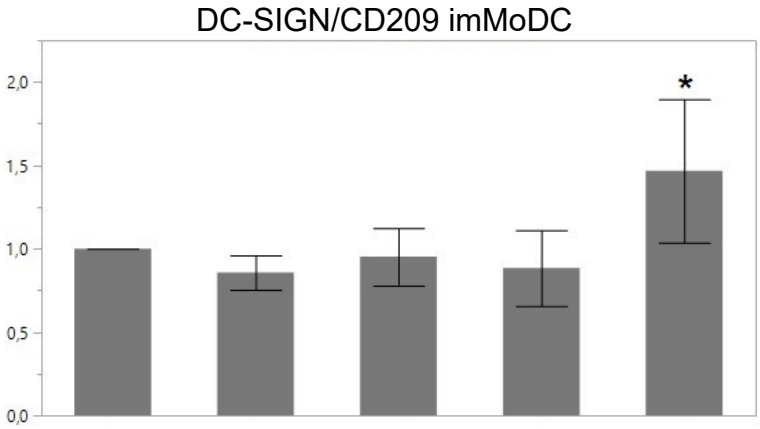

Figure 4.2.3 a: Average and standard deviation of the DMFI in each imMoDC group. The values were normalized to 1.00 for DMSO treated imMoDC. Columns left to right: DMSO, 100 nM carfilzomib, 100 nM Kyprolis, 1 ng/ml=2.6 nM bortezomib/ 24 h, IL-10; y axis: DMFI; asterisks signify statistical significance; N=10

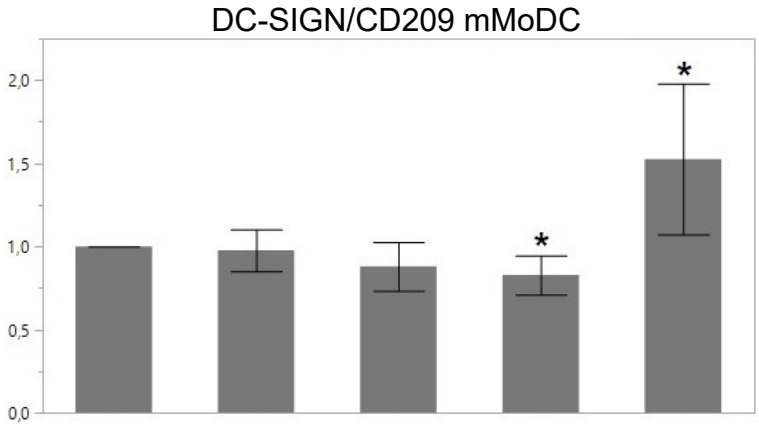

Figure 4.2.3 b: Average and standard deviation of the DMFI in each mMoDC group. The values were normalized to 1.00 for DMSO treated mMoDC. Columns left to right: DMSO, 100 nM carfilzomib, 100 nM Kyprolis, 1 ng/ml=2.6 nM bortezomib/ 24 h, IL-10; y axis: DMFI; asterisks signify statistical significance; N=10

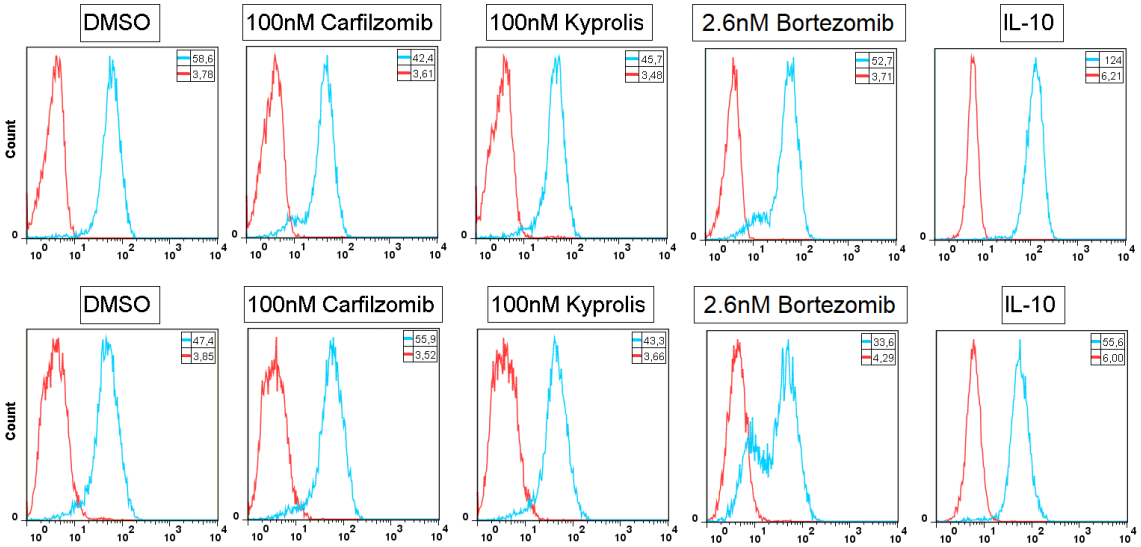

Figure 4.2.3 c: Exemplary overlay of a DC-SIGN/CD209 trial. Top row: imMoDC; bottom row: mMoDC; y axis: cell count; red: IgG-isotype; blue: DC-SIGN/CD209

4.2.4 Exposure to Carfilzomib Decreases Expression of CD83 in LPS Stimulated mMoDC

CD83 is a surface protein that can almost exclusively be found on MoDC which have completed the maturation process. It plays an important role in facilitating T cell immunity and proliferation (see chapter 1.1.5). It was previously shown that bortezomib exposure decreases CD83 expression in LPS stimulated mMoDC and has no effect on its expression in unstimulated imMoDC (65). In this line of experiments, a decrease in CD83 expression average could be observed for the LPS stimulated mMoDC treated

with 30 nM carfilzomib, 100 nM carfilzomib, 100 nM Kyprolis, 1 ng/ml bortezomib/24 h and the IL-10 positive control (see figure 4.2.4 a and c). The decrease of expression was not statistically significant for the 30 nM carfilzomib treatment group (not shown). For every other group the change was significant ($p<0.05$). For bortezomib, this had already been demonstrated in our previous study (65). In imMoDC there was no significant decrease after carfilzomib exposure. Bortezomib exposure caused a statistically significant up-regulation of CD83 in imMoDC, which is not in line with our previous study (see figure 4.2.4 a and b; $p<0.05$).

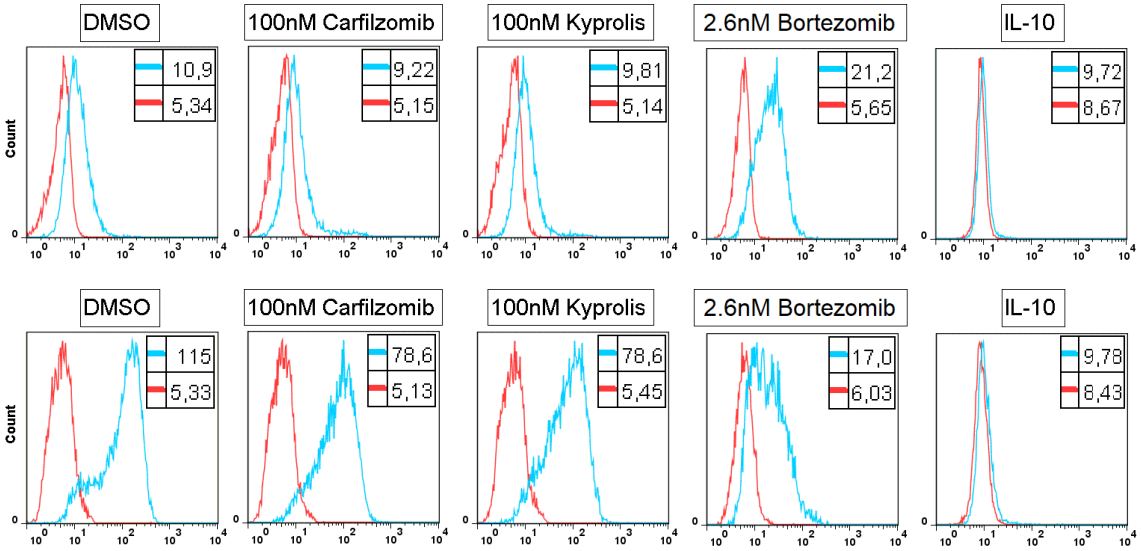

Figure 4.2.4 a: MoDC were stained with a fluorescent anti-CD83, then analysed via flow cytometry. The histograms in this example show a increase in cells with lower expression of CD83 after treatment with carfilzomib and Kyprolis as well as after bortezomib treatment. Top row: imMoDC; bottom row: mMoDC; X-Axis: CD83 expression; y axis: cell count; red: IgG-isotype; blue: CD83

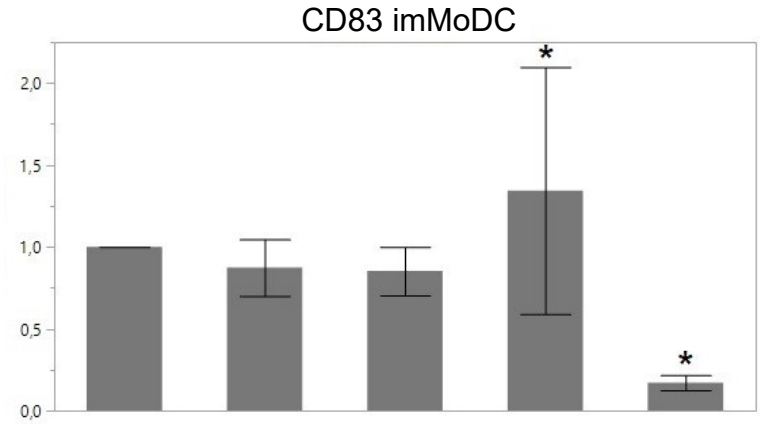

Figure 4.2.4 b: Average and standard deviation of the DMFI in each imMoDC group. The values were normalized to 1.00 for DMSO treated imMoDC. Columns left to right: DMSO, 100 nM carfilzomib, 100 nM Kyprolis, 1 ng/ml=2.6 nM bortezomib/ 24 h, IL-10; y axis: DMFI; asterisks signify statistical significance; N=8

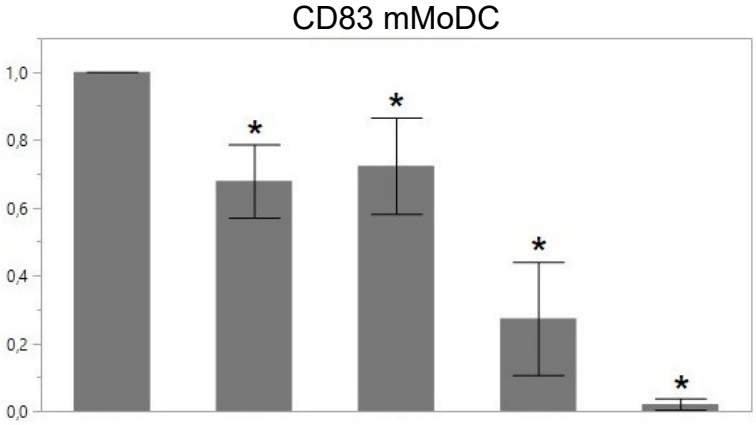

Figure 4.2.4 c: Average and standard deviation of the DMFI in each mMoDC group. The values were normalized to 1.00 for DMSO treated mMoDC. Columns left to right: DMSO, 100 nM carfilzomib, 100 nM Kyprolis, 1 ng/ml=2.6 nM bortezomib/ 24 h, IL-10; y axis: DMFI; asterisks signify statistical significance; N=10

4.2.5 Exposure to Carfilzomib Increases Expression of CD80 in Unstimulated imMoDC but Decreases Its Expression in LPS Stimulated mMoDC

The protein CD80 on the surface of MoDC is an important co-stimulatory molecule for activating T-lymphocytes (see also chapter 1.1.4). It was previously shown that bortezomib exposure decreases CD80 expression in LPS stimulated mMoDC and has no effect on its expression in unstimulated imMoDC (65). In this line of experiments an increased expression of CD80 on average could be observed in all imMoDC treatment groups. This change was statistically significant in the 100 nM carfilzomib, 100 nM Kyprolis and the IL-10 positive control (see figure 4.2.5 b; $p<0.05$). In LPS stimulated mMoDC, the 3 nM carfilzomib treatment group appeared to have increased expression of CD80 which was not statistically significant. In every other treatment group there was a statistically significant decrease in CD80 expression average (see figure 4.2.5 c; $p<0.05$). This has been demonstrated for bortezomib in our previous study (65).

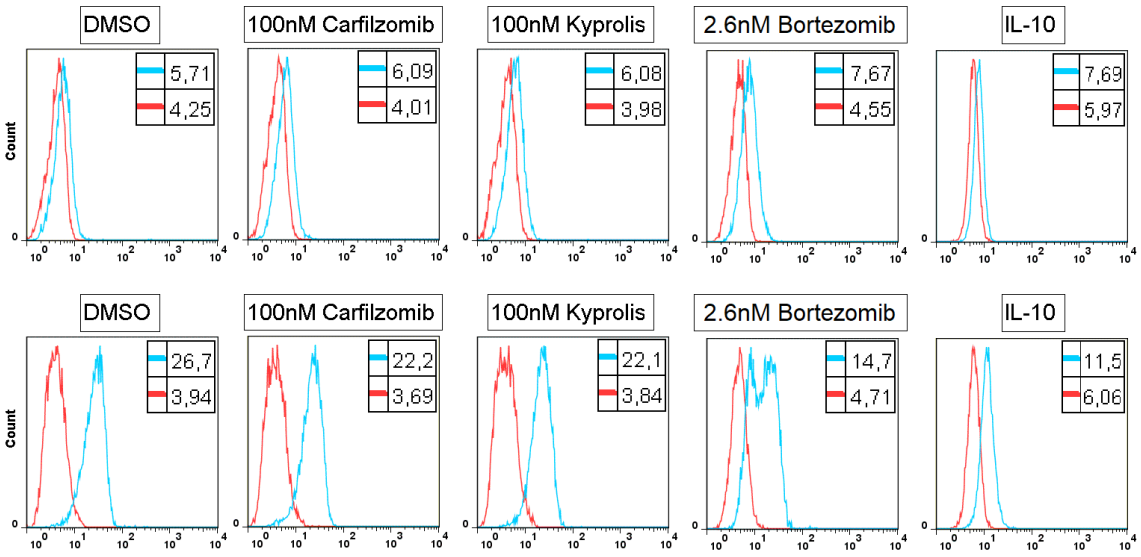

Figure 4.2.5 a: ImMoDC and mMoDC were stained with a fluorescent anti-CD80, then analysed via flow cytometry. The histograms in this example show an increase in imMoDC with higher expression of CD80 after treatment with carfilzomib and Kyprolis as well as an decrease in mMoDC with higher expression of CD80 after carfilzomib, Kyprolis and bortezomib treatment. Top row: imMoDC, bottom row: mMoDC; X-Axis: CD80 expression; y axis: cell count; red: IgG-isotype; blue: CD80

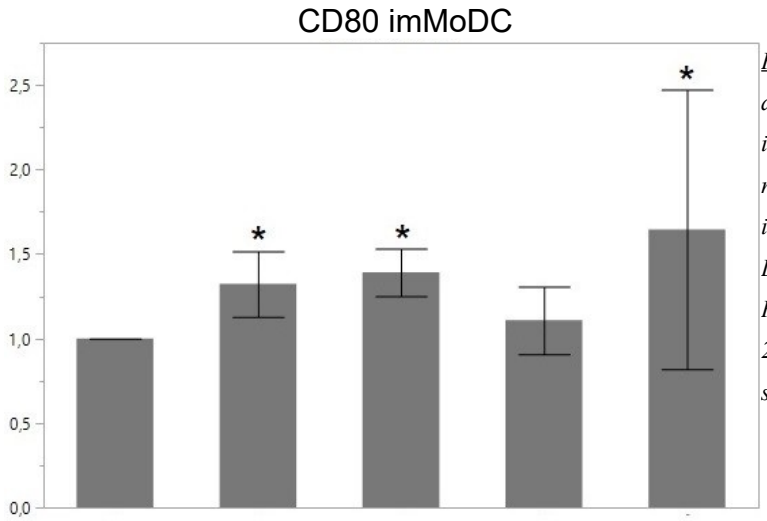

Figure 4.2.5 b: Average and standard deviation of the DMFI in each imMoDC group. The values were normalized to 1.00 for DMSO treated imMoDC. Columns left to right: DMSO, 100 nM carfilzomib, 100 nM Kyprolis, 1 ng/ml=2.6 nM bortezomib/ 24 h, IL-10; y axis: DMFI; asterisks signify statistical significance; N=10

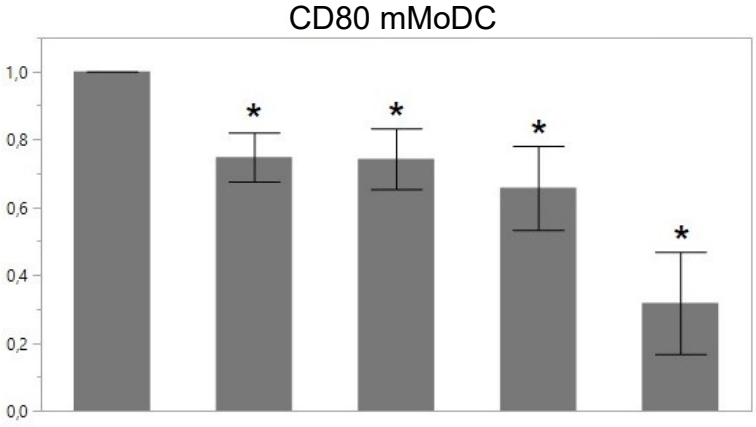

Figure 4.2.5 c: Average and standard deviation of the DMFI in each mMoDC group. The values were normalized to 1.00 for DMSO treated mMoDC. Columns left to right: DMSO, 100 nM carfilzomib, 100 nM Kyprolis, 1 ng/ml=2.6 nM bortezomib/ 24 h, IL-10; y axis: DMFI; asterisks signify statistical significance; N=10

4.2.6 Exposure to Carfilzomib Does Not Affect the Expression of CD86 in Unstimulated or LPS Stimulated MoDC

CD86 and CD80 both act as ligands for CD28 and are therefore important for priming T cells (see also chapter 1.1.4). Neither carfilzomib nor Kyprolis had a statistically significant effect on the expression of CD86 in unstimulated or LPS stimulated mMoDC (see figure 4.2.6 a and b; $p>0.05$) while bortezomib exposure resulted in a statistically significant decrease of CD86 expression in LPS stimulated mMoDC (see figure 4.2.6 b; $p<0.05$) which is in line with our previous study (65).

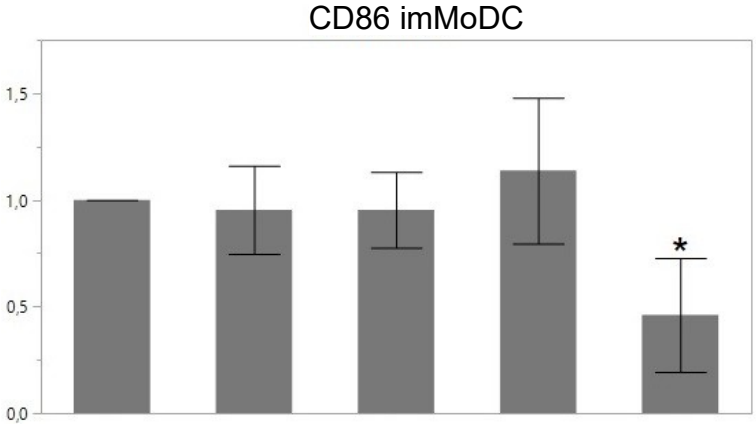

Figure 4.2.6 a: Average and standard deviation of the DMFI in each imMoDC group. The values were normalized to 1.00 for DMSO treated imMoDC. Columns left to right: DMSO, 100 nM carfilzomib, 100 nM Kyprolis, 1 ng/ml=2.6 nM bortezomib/ 24 h, IL-10; y axis: DMFI; asterisks signify statistical significance; N=9

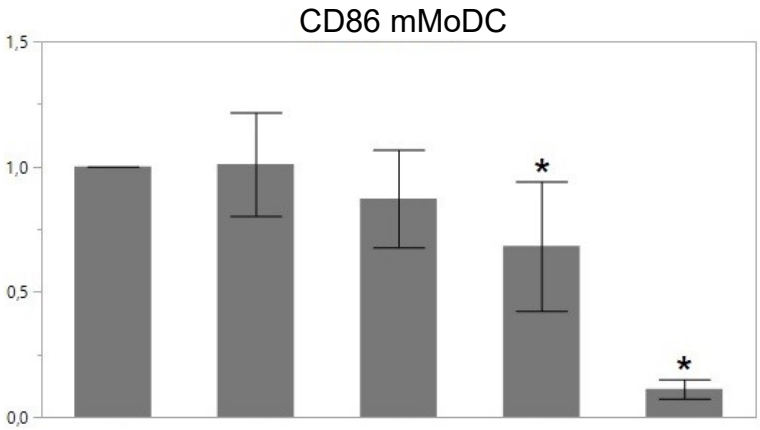

Figure 4.2.6 b: Average and standard deviation of the DMFI in each mMoDC group. The values were normalized to 1.00 for DMSO treated mMoDC. Columns left to right: DMSO, 100 nM carfilzomib, 100 nM Kyprolis, 1 ng/ml=2.6 nM bortezomib/ 24 h, IL-10; y axis: DMFI; asterisks signify statistical significance; N=10

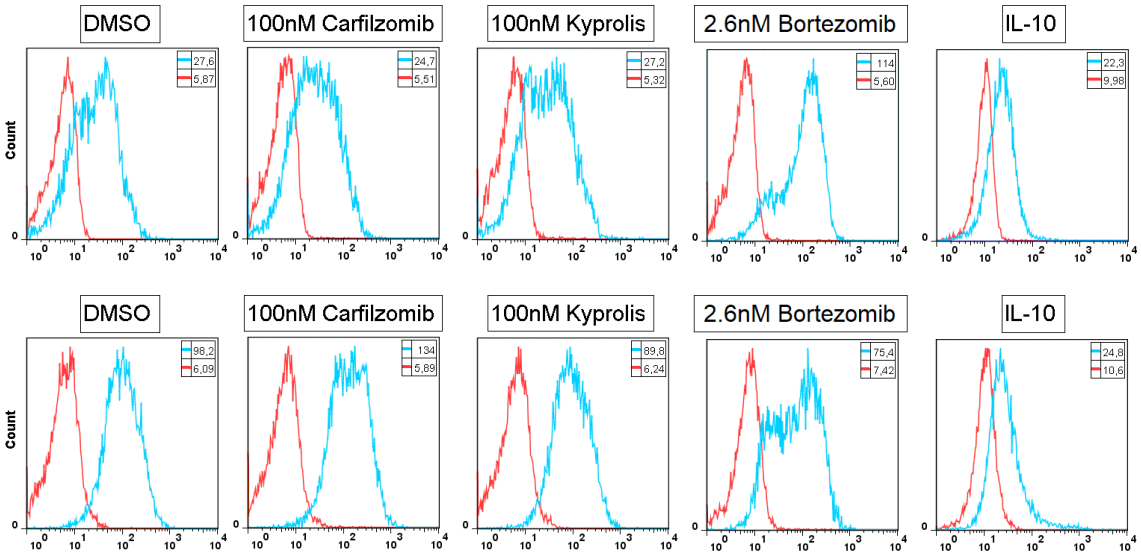

Figure 4.2.6 c: Exemplary overlay of a CD86 trial. Top row: imMoDC; bottom row: mMoDC; y axis: cell count; red: IgG-isotype; blue: CD86

4.2.7 Exposure to Carfilzomib Does Not Affect the Expression of HLA-DR in Unstimulated or LPS Stimulated MoDC

Carfilzomib and Kyprolis exposure had no statistically significant effect on the expression of the peptide presenting MHC Type II molecule HLA-DR in unstimulated or LPS stimulated mMoDC. Exposure to bortezomib produced a statistically significant decrease of HLA-DR expression in unstimulated and LPS stimulated mMoDC (see figure 4.2.7 a and b; $p<0.05$). For mMoDC, but not for imMoDC, this has been demonstrated in our previous study (65).

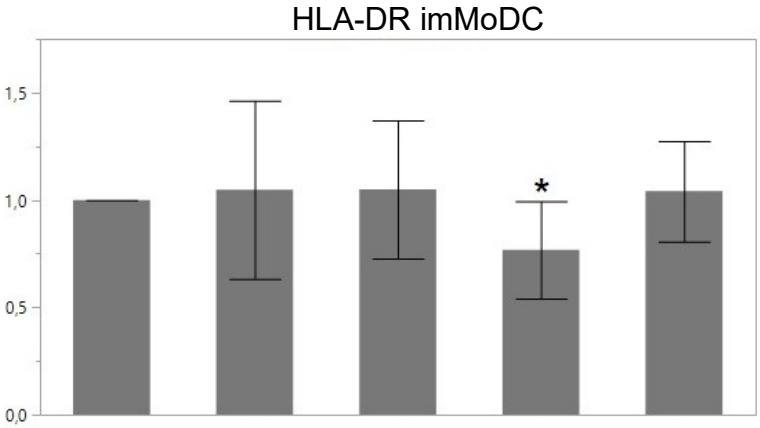

Figure 4.2.7 a: Average and standard deviation of the DMFI in each imMoDC group. The values were normalized to 1.00 for DMSO treated imMoDC. Columns left to right: DMSO, 100 nM carfilzomib, 100 nM Kyprolis, 1 ng/ml=2.6 nM bortezomib/ 24 h, IL-10; y axis: DMFI; asterisks signify statistical significance; N=10

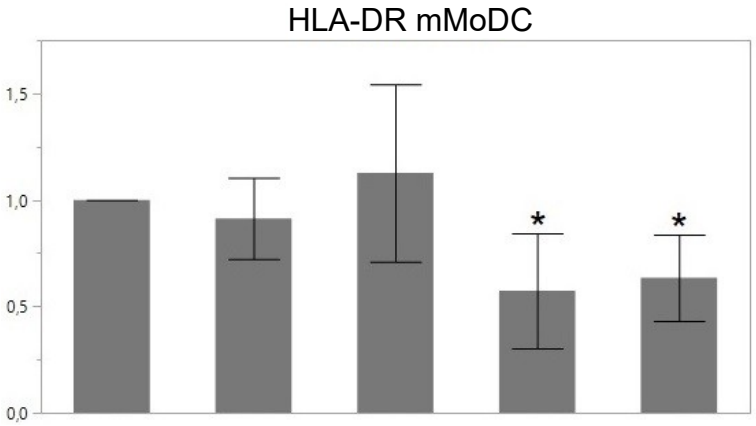

Figure 4.2.7 b: Average and standard deviation of the DMFI in each mMoDC group. The values were normalized to 1.00 for DMSO treated mMoDC. Columns left to right: DMSO, 100 nM carfilzomib, 100 nM Kyprolis, 1 ng/ml=2.6 nM bortezomib/ 24 h, IL-10; y axis: DMFI; asterisks signify statistical significance; N=9

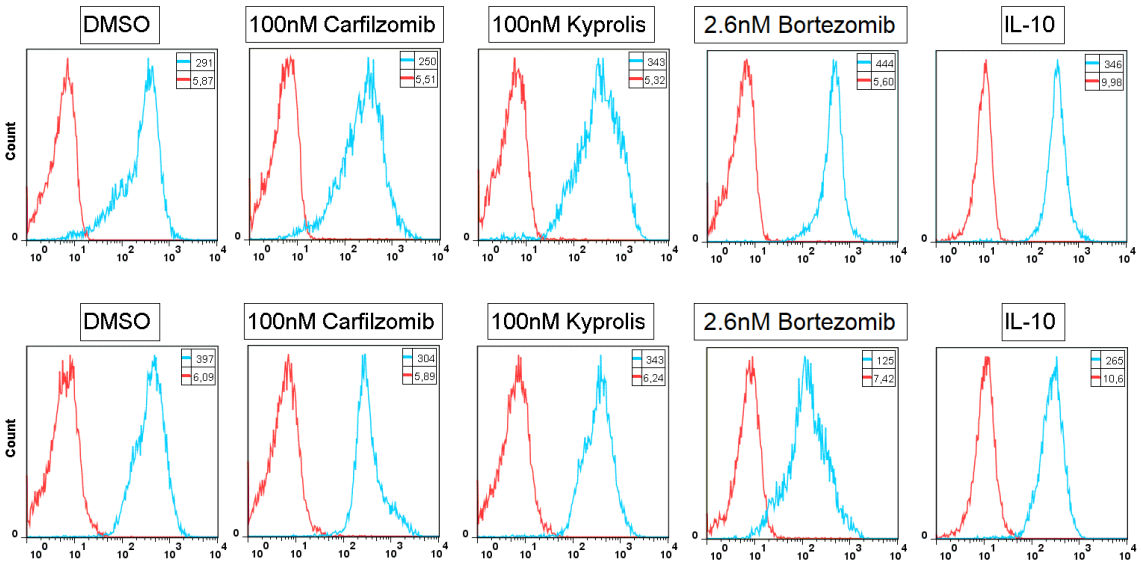

Figure 4.2.7 c: Exemplary overlay of a HLA-DR trial. Top row: imMoDC; bottom row: mMoDC; y axis: cell count; red: IgG-isotype; blue: HLA-DR

4.2.8 Exposure to Carfilzomib Increases the Expression of CCR7 in Unstimulated and LPS Stimulated MoDC

CCR7 is an important receptor for cell migration towards lymph nodes (81). In imMoDC, 100 nM carfilzomib, but not Kyprolis, produced a statistically significant increase in CCR7 surface expression (see figure 4.2.8 a; $p<0.05$) while the increase in mMoDC was not significant (see figure 4.2.8 b; $p>0.05$). Bortezomib exposure produced a statistically significant decrease in LPS stimulated mMoDC (see figure 4.2.8 b; $p<0.05$) which has also been demonstrated in our previous study (65).

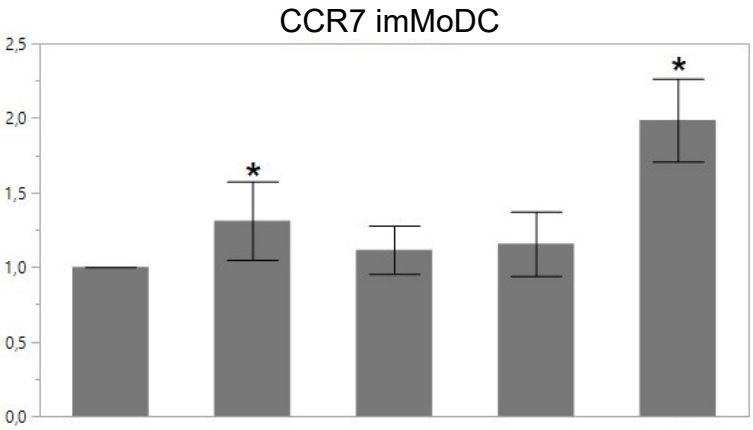

Figure 4.2.8 a: Average and standard deviation of the DMFI in each imMoDC group. The values were normalized to 1.00 for DMSO treated imMoDC. Columns left to right: DMSO, 100 nM carfilzomib, 100 nM Kyprolis, 1 ng/ml=2.6 nM bortezomib/ 24 h, IL-10; y axis: DMFI; asterisks signify statistical significance; N=6

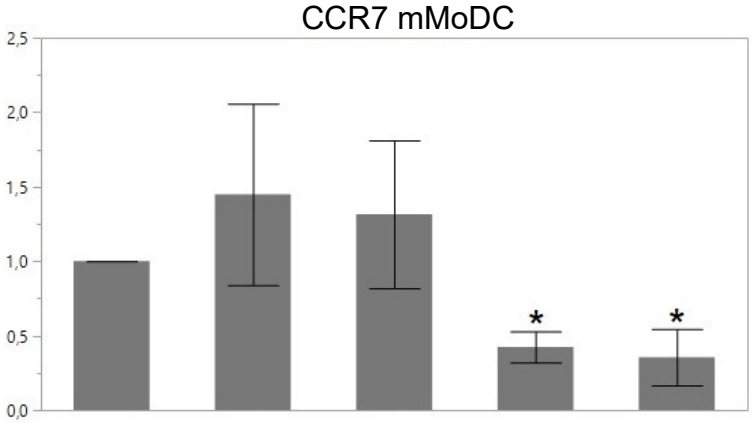

Figure 4.2.8 b: Average and standard deviation of the DMFI in each mMoDC group. The values were normalized to 1.00 for DMSO treated mMoDC. Columns left to right: DMSO, 100 nM carfilzomib, 100 nM Kyprolis, 1 ng/ml=2.6 nM bortezomib/ 24 h, IL-10; y axis: DMFI; asterisks signify statistical significance; N=6

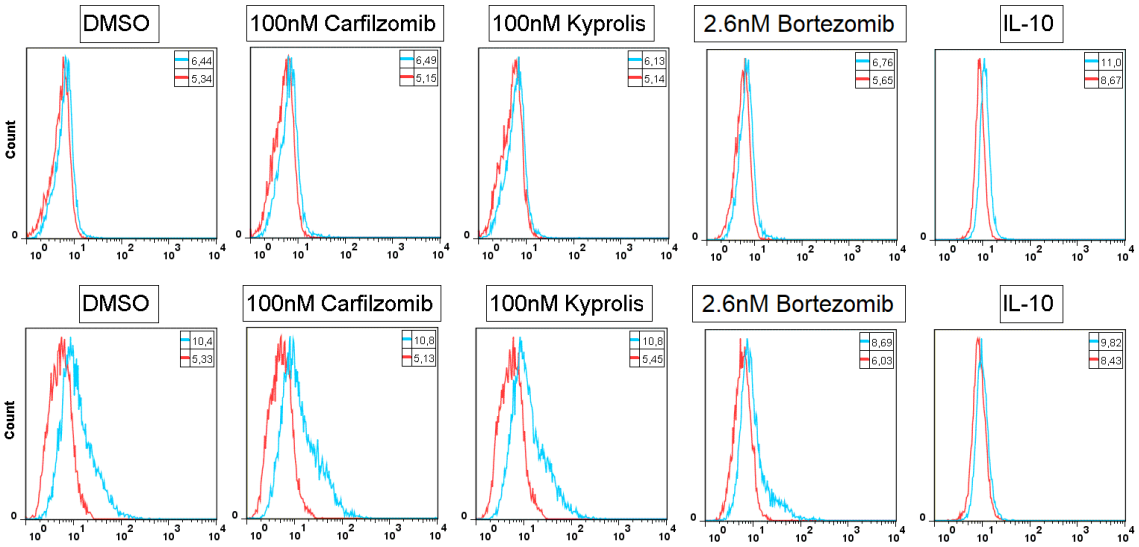

Figure 4.2.8 c: Exemplary overlay of a CCR7 trial. Top row: imMoDC; bottom row: mMoDC; y axis: cell count; red: IgG-isotype; blue: CCR7

4.2.9 Exposure to Carfilzomib Does Not Affect the Expression of GPNMB/Osteoactivin in Unstimulated or LPS Stimulated MoDC

GPNMB/Osteoactivin is a transmembrane protein, which acts as a coinhibitory molecule strongly inhibiting T cell responses if present on APC. Our working group has previously shown that its expression on human MoDC is dramatically upregulated upon treatment with IL-10 but also by BCR-ABL tyrosine kinase inhibitors (82). Neither bortezomib, nor carfilzomib or Kyprolis had a statistically significant effect on its expression in unstimulated or LPS stimulated mMoDC (see figure 4.2.9 a and b; $p>0.05$).

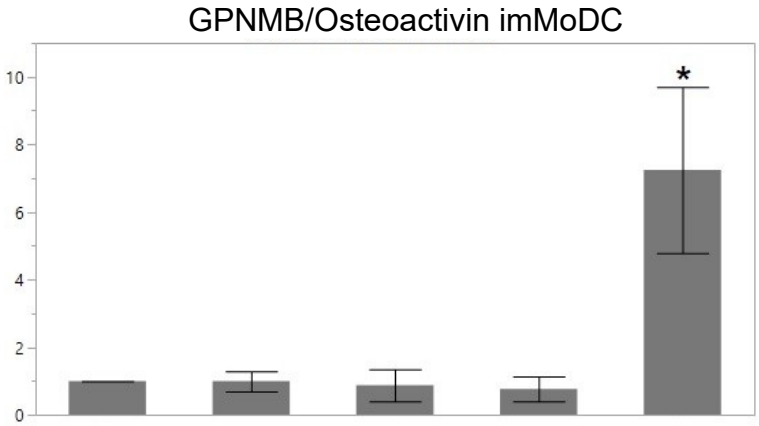

Figure 4.2.9 a: Average and standard deviation of the DMFI in each imMoDC group. The values were normalized to 1.00 for DMSO treated imMoDC. Columns left to right: DMSO, 100 nM carfilzomib, 100 nM Kyprolis, 1 ng/ml=2.6 nM bortezomib/ 24 h, IL-10; y axis: DMFI; asterisks signify statistical significance; N=3

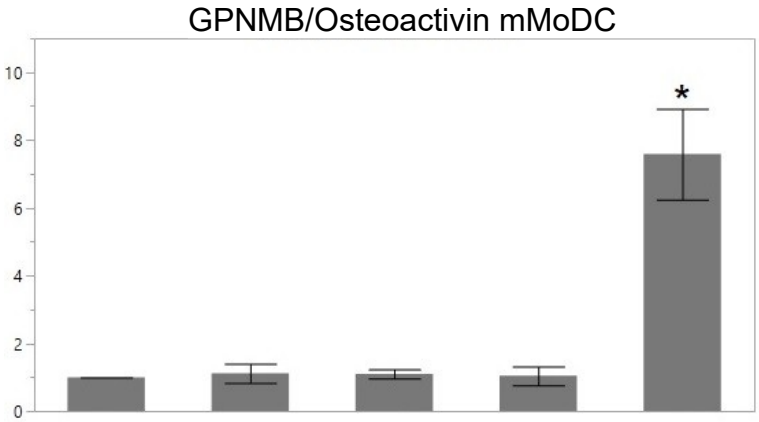

Figure 4.2.9 b: Average and standard deviation of the DMFI in each mMoDC group. The values were normalized to 1.00 for DMSO treated mMoDC. Columns left to right: DMSO, 100 nM carfilzomib, 100 nM Kyprolis, 1 ng/ml=2.6 nM bortezomib/ 24 h, IL-10; y axis: DMFI; asterisks signify statistical significance; N=3

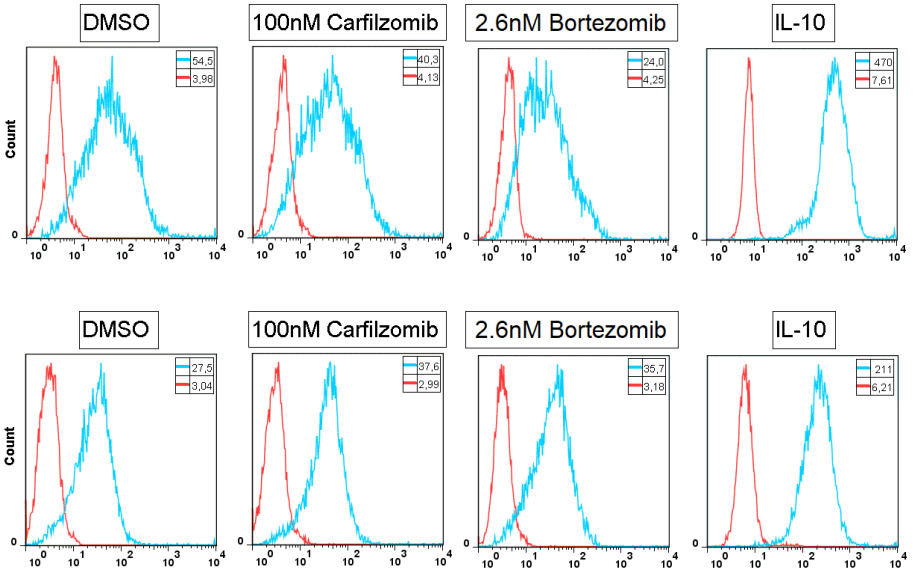

Figure 4.2.9 c: Exemplary overlay of an GPNMB/Osteoactivin trial. Top row: imMoDC; bottom row: mMoDC; y axis: cell count; red: IgG-isotype; blue: osteoactivin

4.3 MoDC Function

Carfilzomib Does Not Significantly Impair Migration of MoDC

The ability to migrate is an important requirement for DC to fulfill their purpose of stimulating T cells in the lymph nodes. The migration assay and subsequent analysis via flow cytometry did not show a statistically significant change in migratory capacity of imMoDC or mMoDC after exposure to 100 nM of either carfilzomib or Kyprolis (see

figure 4.3 a and b; $p>0.05$). Exposure to 1 ng/ml bortezomib for 24 h lowered the migratory capacity of LPS stimulated mMoDC to a statistically significant extent which is consistent with the results of our previous study (see figure 4.3 b; $p<0.05$).

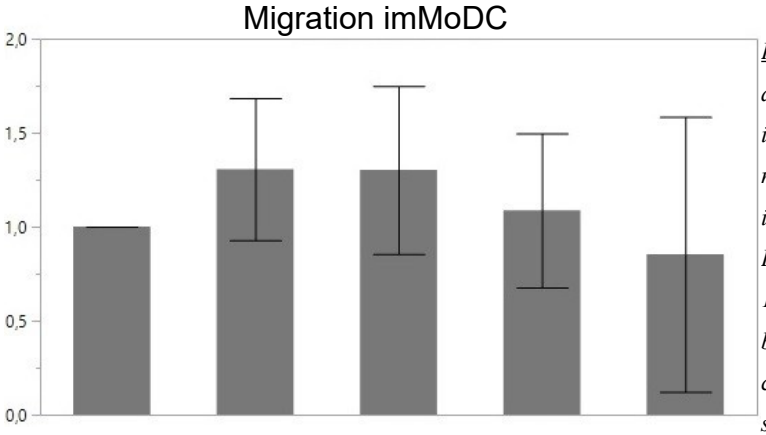

Figure 4.3 a: Average and standard deviation of the cell count in each imMoDC group. The values were normalized to 1.00 for DMSO treated imMoDC. Columns left to right: DMSO, 100 nM carfilzomib, 100 nM Kyprolis, 1 ng/ml=2.6 nM bortezomib/24 h, IL-10; y axis: cell count; asterisks signify statistical significance; N=8

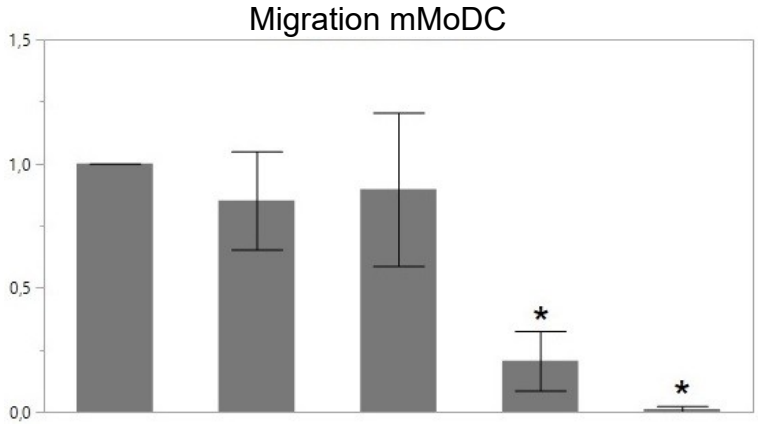

Figure 4.3 b: Average and standard deviation of the cell count in each mMoDC group. The values were normalized to 1.00 for DMSO treated mMoDC. Columns left to right: DMSO, 100 nM carfilzomib, 100 nM Kyprolis, 1 ng/ml=2.6 nM bortezomib/24 h, IL-10; y axis: cell count; asterisks signify statistical significance; N=9

4.4 MoDC Cytokine Secretion

Carfilzomib Affects Cytokine Levels to a Lesser Extent Than Bortezomib

After stimulation and during their maturation process, DC undergo functional changes. One significant change is the increased secretion of inflammatory cytokines (see chapter 1.1.5). We analysed levels of IL-6, IL-12, MCP-1/CCL2, MIP-1α/CCL3 and Rantes/CCL5 with ELISA assays. The results of these experiments were not statistically significant except for a decrease in imMoDC MCP-1/CCL2 concentration and mMoDC MIP-1α (see figures 4.4.1 b and 4.4.2 a).

The tendency towards lower cytokine concentrations after bortezomib exposure in LPS stimulated mMoDC is in line with our prevous study.

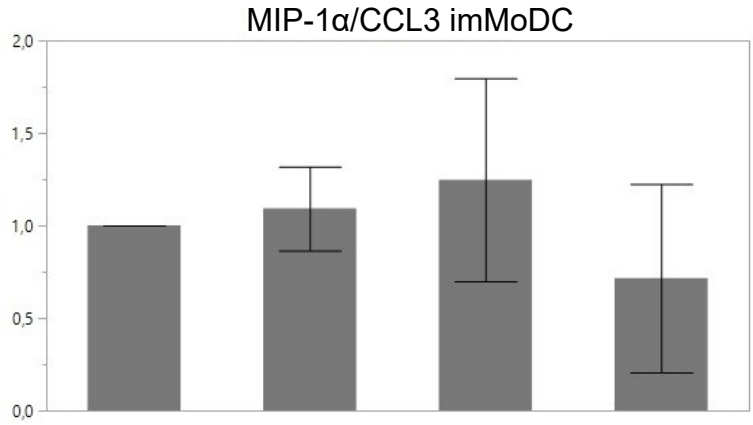

Figure 4.4.1 a: Average and standard deviation in the supernatant cytokine concentration of the imMoDC group. The values were normalized to 1.00 for DMSO treated imMoDC. Columns left to right: DMSO, 100 nM carfilzomib, 100 nM Kyprolis, 1 ng/ml=2.6 nM bortezomib/24 h; y axis: concentration; asterisks signify statistical significance; N=5

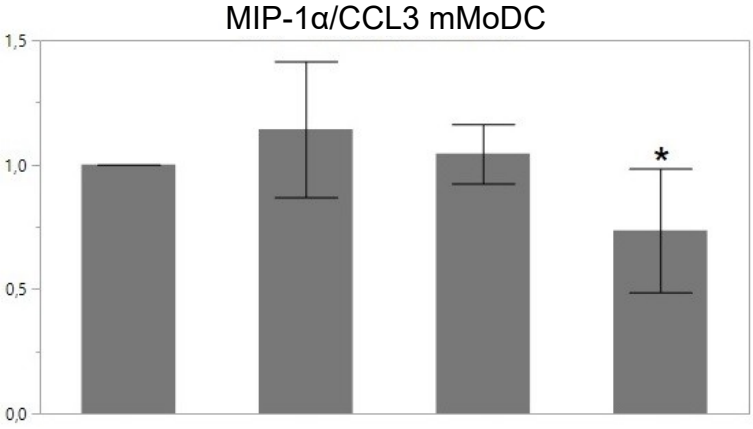

Figure 4.4.1 b: Average and standard deviation in the supernatant cytokine concentration of the mMoDC group. The values were normalized to 1.00 for DMSO treated mMoDC. Columns left to right: DMSO, 100 nM carfilzomib, 100 nM Kyprolis, 1 ng/ml=2.6 nM bortezomib/24 h; y axis: concentration; asterisks signify statistical significance; N=7

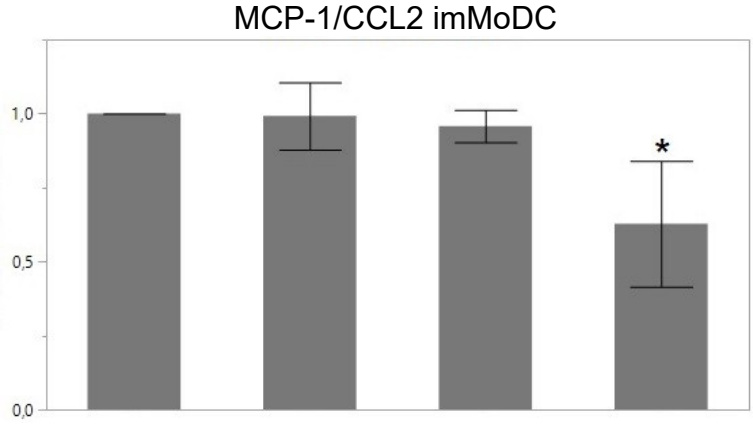

Figure 4.4.2 a: Average and standard deviation in the supernatant cytokine concentration of the imMoDC group. The values were normalized to 1.00 for DMSO treated imMoDC. Columns left to right: DMSO, 100 nM carfilzomib, 100 nM Kyprolis, 1 ng/ml=2.6 nM bortezomib/24 h; y axis: concentration; asterisks signify statistical significance; N=5

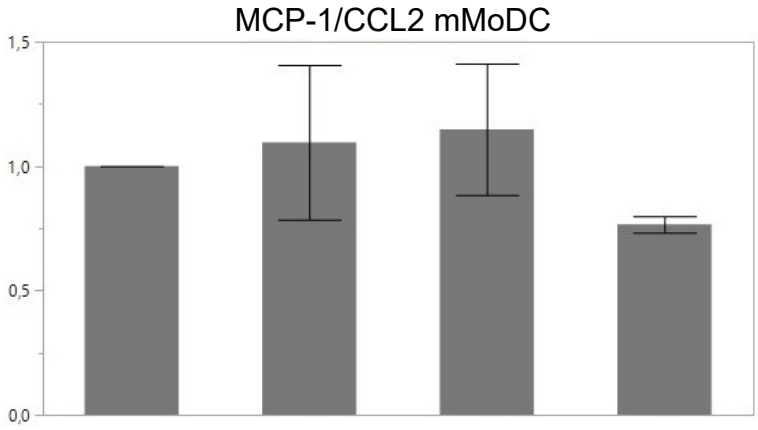

Figure 4.4.2 b: Average and standard deviation in the supernatant cytokine concentration of the mMoDC group. The values were normalized to 1.00 for DMSO treated mMoDC. Columns left to right: DMSO, 100 nM carfilzomib, 100 nM Kyprolis, 1 ng/ml=2.6 nM bortezomib/24 h; y axis: concentration; asterisks signify statistical significance; N=5

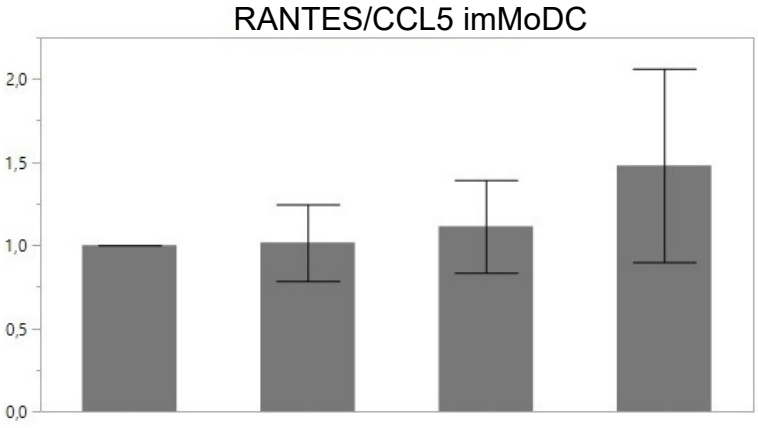

Figure 4.4.3 a: Average and standard deviation in the supernatant cytokine concentration of the imMoDC group. The values were normalized to 1.00 for DMSO treated imMoDC. Columns left to right: DMSO, 100 nM carfilzomib, 100 nM Kyprolis, 1 ng/ml=2.6 nM bortezomib/24 h; y axis: concentration; asterisks signify statistical significance; N=5

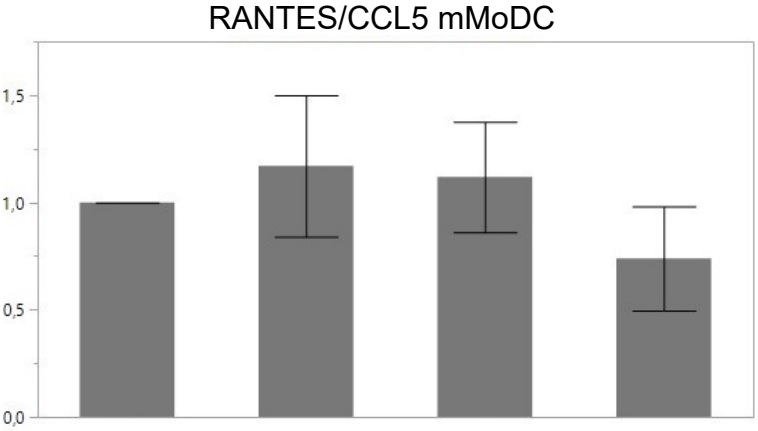

Figure 4.4.3 b: Average and standard deviation in the supernatant cytokine concentration of the mMoDC group. The values were normalized to 1.00 for DMSO treated mMoDC. Columns left to right: DMSO, 100 nM carfilzomib, 100 nM Kyprolis, 1 ng/ml=2.6 nM bortezomib/24 h; y axis: concentration; asterisks signify statistical significance; N=8

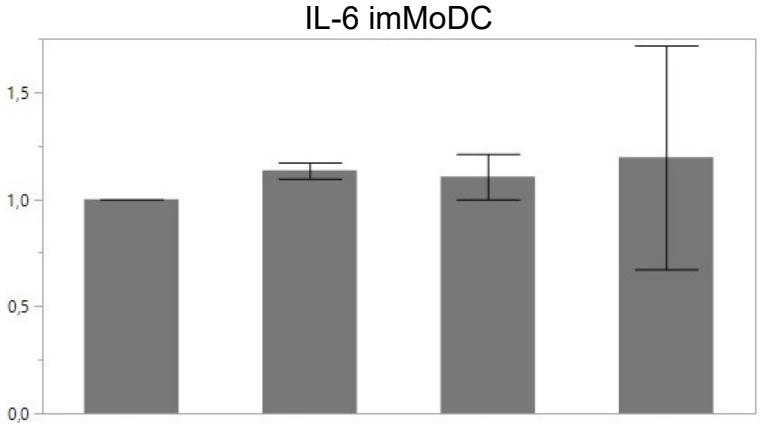

Figure 4.4.4 a: Average and standard deviation in the supernatant cytokine concentration of the imMoDC group. The values were normalized to 1.00 for DMSO treated imMoDC. Columns left to right: DMSO, 100 nM carfilzomib, 100 nM Kyprolis, 1 ng/ml=2.6 nM bortezomib/24 h; y axis: concentration; asterisks signify statistical significance; N=5

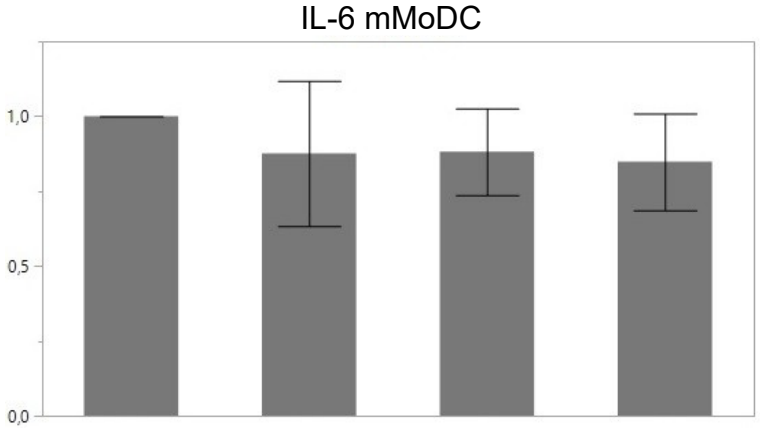

Figure 4.4.4 b: Average and standard deviation in the supernatant cytokine concentration of the mMoDC group. The values were normalized to 1.00 for DMSO treated mMoDC. Columns left to right: DMSO, 100 nM carfilzomib, 100 nM Kyprolis, 1 ng/ml=2.6 nM bortezomib/24 h; y axis: concentration; asterisks signify statistical significance; N=5

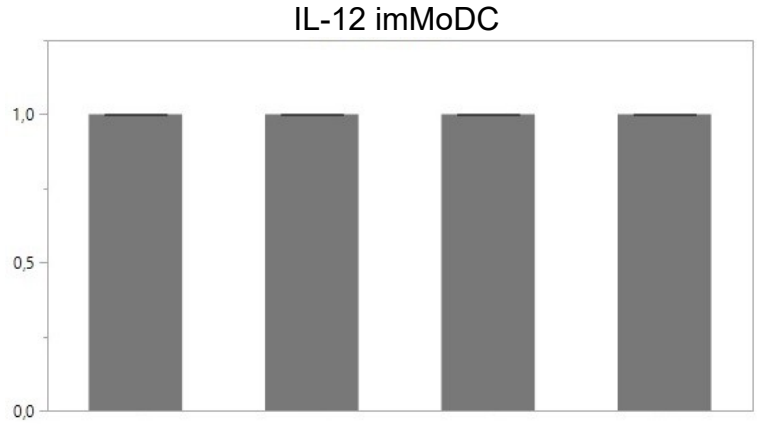

Figure 4.4.5 a: Average and standard deviation in the supernatant cytokine concentration of the imMoDC group. The values were normalized to 1.00 for DMSO treated imMoDC. Columns left to right: DMSO, 100 nM carfilzomib, 100 nM Kyprolis, 1 ng/ml=2.6 nM bortezomib/24 h; y axis: concentration; asterisks signify statistical significance; N=5

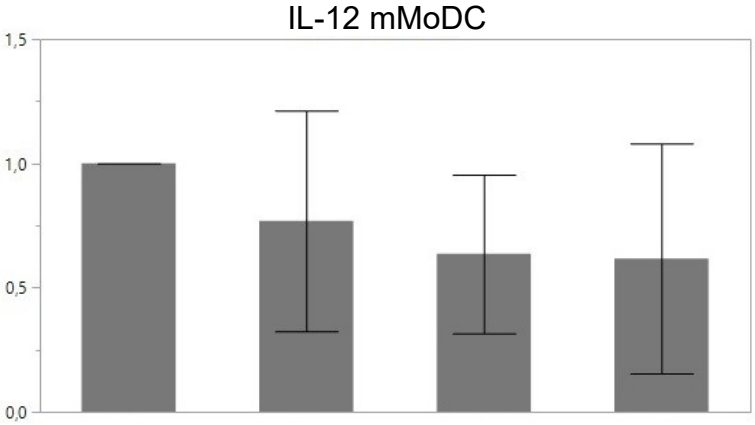

Figure 4.4.5 b: Average and standard deviation in the supernatant cytokine concentration of the mMoDC group. The values were normalized to 1.00 for DMSO treated mMoDC. Columns left to right: DMSO, 100 nM carfilzomib, 100 nM Kyprolis, 1 ng/ml=2.6 nM bortezomib/24 h; y axis: concentration; asterisks signify statistical significance; N=7

5. Discussion

As crucial facilitators of communication between innate and adaptive immunity, DC have been endowed with a comparatively large variety of abilities, several of which have been examined in this project. Some DC subtypes in peripheral blood are very rare and difficult to cultivate in monocultures, which is the reason why this project focused on MoDC.

Many of the available cancer and myeloma drugs are non-selective and have severe side effects. Nowadays, despite several modes of treatment being available, multiple myeloma remains incurable in most cases. We used this *in vitro* model to examine the effects of carfilzomib on MoDC to asses the viability of a combined approach to myeloma treatment, which has the potential to mitigate the severe side effects of current tumour therapy regimens by using vaccination to achieve the goal of a long-term immune response and disease remission. Nencioni *et al.* had previously demonstrated several detrimental effects of bortezomib on MoDC function: It affected MoDC activation and viability (64), caused reduced levels of RelB[2], reduced levels of phosphorylated p42/ERK2 belonging to the MAP kinases and interferon regulatory factor pathway as well as decreased expression of MyD88 which interacts with MAP kinases and NF-κB pathway activating kinases; skewed phenotypic maturation, a decline in migration towards CCL19/MIP-3β, lower stimulatory capacity and less secretion of IL-12 and TNF were also observed (65). In imMoDC, bortezomib exposure resulted in lower endocytic capacity and less expression of the CD206 mannose receptor (65).

The study was designed to contrast the previously demonstrated effects of proteasome inhibition via bortezomib on MoDC to that of proteasome inhibition via carfilzomib with IL-10 serving as a positive control. LPS is an archetypal DC stimulus and induces a phenotypic activation via the TLR4 and NF-kB signal transduction pathway. Therefore it was used as maturation stimulus despite its bacterial origin because it causes the desired response with increased secretion of inflammatory IL-12 and T cell

2 A transcription factor interacting with NF-κB.

differentiation leaning towards T_{h1} cells which then leads to the increased $CD8^+$ T cell and NK cell toxicity desirable for a potential tumour therapy (83).

To find a suitable carfilzomib dosage for the MoDC functional analysis we conducted cell viability assays and found that 300 nM carfilzomib would be too toxic and used 100 nM instead which yielded better results (see chapter 4.1.1). For bortezomib we chose a dosage that had affected the MoDC phenotype in previous publications.

We also compared the *in vitro* anti-myeloma effect of bortezomib and carfilzomib on the U266 multiple myeloma cell line and found rates of apoptosis ranging from 74.8 % to 96.6 % for the 100 nM carfilzomib group, 54.2 % to 79.8 % for the 100 nM Kyprolis group and 16.3 % to 32.6 % for the 1 ng/ml (2.6 nM) bortezomib group. The main difference between 100 nM and 300 nM carfilzomib exposure was the percentage of cells which had already progressed from early to late apoptosis at the time of analysis. There seemed to be no noticeable difference in induction of apoptosis between 1000 nM carfilzomib and 300 nM carfilzomib. The 30 nM carfilzomib dosage was inferior to higher dosages with regard to induction of apoptosis. 100 nM of the medical grade Kyprolis seemed to be slightly inferior to the chemical compound. These results suggest bortezomib being inferior to carfilzomib in terms of *in vitro* anti-myeloma effect in a dosage which is already detrimental to MoDC function. Minor differences between the two types of carfilzomib can be explained by the fact that samples of the medical grade carfilzomib could only be obtained after a patient's intravenous infusion had been completed and the fluid remaining in the infusion tube could be extracted. At that time, the drug had been exposed to light and room temperature, which may have slightly lowered the amount of active molecules. Another possible explanation would be the medical grade carfilzomib being dissolved in 5 % glucose solution and the non-medical grade agent being dissolved in DMSO.

Carfilzomib caused some statistically significant changes to the MoDC phenotype. However, the changes were considerably less pronounced than the ones caused by its predecessor bortezomib despite its comparatively higher apoptotic effect in the myeloma cell culture. The DMSO treated MoDC yielded populations with the regular phenotype and could therefore be used as the reference to which other treatment groups

had to be compared. Except for IL-10 which caused a statistically significant increase, CD14 expression remained almost unchanged for all substances as would be expected after successful differentiation into MoDC. DC-SIGN/CD209 and CD1a as DC markers were not affected by carfilzomib while bortezomib caused a statistically significant down-regulation in both. Expression of the antigen-presentation molecule HLA-DR was unaffected by carfilzomib but negatively affected by bortezomib exposure to a statistically significant extent.

In imMoDC carfilzomib and Kyprolis exposure caused a statistically significant up-regulation of CD80. This, however, was a minor change to a low level of expression and might therefore be irrelevant. In mMoDC carfilzomib and Kyprolis exposure caused a statistically significant down-regulation of CD80 and CD83.

Bortezomib exposure caused a statistically significant up-regulation of CD83 in imMoDC and a statistically significant down-regulation of CD80 and CD83 in mMoDC. In the imMoDC carfilzomib groups, CD80 was up-regulated to a statistically significant extent. DC that show a disparity in functional maturation have been described as semi-mature with an up-regulation of co-stimulatory molecules without any relevant cytokine secretion and have been reported to cause T cell anergy (84). Since this may cause vaccines to be less effective, further research would be required to determine whether this effect is substantial enough to increase the tolerogenic effect of iDC. Additional research into this might also be useful in the context of possible treatments for autoimmune diseases.

Down-regulation of CD83 in DC has been associated with lower capacity to prime $CD8^+$ T cells for specific tumour antigens, with less induction T cell proliferation and a decrease in T cell IFN-γ secretion (15). As this would be undesirable when using vaccines, carfilzomib may be less adverse in a combined therapeutic approach than bortezomib because the effect on CD83 expression was much weaker than that of its predecessor. Looking at the expression of CD80 – an important co-stimulatory molecule for T cell activation – the difference between the two substances was less pronounced. Bortezomib exposure also caused a statistically significant down-regulation of CD1a and HLA-DR in imMoDC and a statistically significant down-regulation of all analysed

surface molecules except osteoactivin in mMoDC. Carfilzomib exposure also caused a statistically significant up-regulation of CCR7 which did not result in a noticeable increase in migrated cells.

All findings regarding the mMoDC phenotype after bortezomib exposure are consistent with our previous publications (65).

Bortezomib was almost similar to IL-10 in the mMoDC migration assay while carfilzomib did not significantly change the CCR7-mediated migration when compared to untreated cells. This is especially desirable when using non-cellular vaccines meant to stimulate DC *in vivo*. *Ex vivo* generated DC may have little to no carfilzomib exposure, and that is why this finding may be less relevant for those vaccines.

Analysis of MoDC cytokine secretion showed a statistically significant decrease in imMoDC MCP-1/CCL2 concentration and mMoDC MIP-1α/CCL3 concentration after bortezomib exposure. Rantes/CCL5 and the aforementioned cytokines are important factors produced at inflammation sites (85–87). One of their main functions is attracting and recruiting additional leukocytes. In contrast to that, IL-6 and IL-12 are cytokines of systemic inflammation and therefore complex in their functions (88, 89). For all cytokines analysed, a consistent trend of higher cytokine expression for LPS stimulated mMoDC after carfilzomib or Kyprolis exposure in comparison to bortezomib exposure could be observed. The results were not statistically significant but lower cytokine concentration after bortezomib exposure is in keeping with our previous results (65). These results not being statistically significant may be a donor-dependent phenomenon or due to the number of experiments performed. There have been previous studies with conflicting results regarding MoDC function after bortezomib exposure: Some confirm the drug having a detrimental effect on different aspects of MoDC function (65, 90) while other results provide evidence for an augmented DC driven immune response to different tumour entities after exposure to it (91). *In vivo* experiments seem to support the former (92) which makes the discussion about using proteasome inhibitors for immunomodulation a controversial one. There is also evidence suggesting a clinical benefit using bortezomib in the treatment of graft-versus-host disease which might originate from its modulating effect on DC function and its potential to attenuate

immune reactions (93, 94).

Systemic therapy of multiple myeloma could certainly be the origin of DC dysfunction but the disease itself has similar potential to be the cause. It has been reported that plasmacytoid and myeloid DC accumulate in the bone marrow where the myeloid DC interact with CD28 on myeloma cells which causes the tumour cells to down-regulate expression of intracellular proteasome structures associated with HLA type I and thereby lead to myeloma cells more easily avoiding $CD8^+$ T cell killing (66). One could speculate this to be a reason for the so far unsatisfactory results of vaccination in multiple myeloma therapy. Abatacept, a CTLA-4 fusion protein which competitively inhibits CD80/CD86 binding to CD28 and is primarily used to treat rheumatoid arthritis (95), is already being incorporated in current studies (96) to offset the resistance to chemotherapy which is also facilitated by CD28 expressed on myeloma cells (97) and could lead to better patient outcomes not just because of better response to chemotherapy but also to tumour vaccines. Carfilzomib does not specifically target multiple myeloma cells and could therefore be used in treatment regimens for other tumours. An anti-tumour effect against mantle cell lymphoma has been demonstrated *in vitro* and in a mouse model (98). Some breast cancer cell lines also responded well to carfilzomib in combination with other treatments *in vitro* (99–101). Pre-clinical trials with carfilzomib in anaplastic thyroid cancer, non-small-cell lung cancer as well as small-cell lung cancer and colorectal cancer (102–104) have been somewhat promising as well as models with improved micellar carfilzomib in non-small-cell lung cancer cell lines and multiple myeloma (105). The results of this project would therefore also be pertinent when considering combined immunotherapeutic approaches, e.g. in non-small-cell lung cancer (106).

Other effects of proteasome inhibition via carfilzomib include micro-environmental changes through induction of apoptosis in cancer associated fibroblasts of other cancer entities (107) as well as the aforementioned alteration of the HLA-presented peptidome (see chapter 1.3) which was demonstrated by Kowalewski *et al.* using the same time of exposure to and concentration of carfilzomib that was used in this project (68). To be able to estimate possible clinical benefits of myeloma vaccines in patients undergoing

carfilzomib treatment, effects of the altered peptidome on the immunogenicity of multiple myeloma cells have yet to be analysed.

To this day most types of cancer present a therapeutic challenge. Most patients in advanced stages can neither receive a definitive cure nor can their disease be perpetually stabilized. The immune system is an important part of what has to be a multimodal approach to treating a very heterogeneous disease.

In this project we have established that carfilzomib, as opposed to bortezomib, has very little effect on the phenotype of MoDC *in vitro*. Its effect on MoDC function with regard to cytokine secretion and migration compares favourably to its predecessor. This suggests that combining tumour vaccination with carfilzomib may be more viable than using bortezomib in this manner. It also suggests that the immune system in patients treated with carfilzomib may be less iatrogenically compromised than in patients treated with bortezomib. T cell assays analysing the de facto allostimulatory function of MoDC after carfilzomib exposure could be conducted for further research into possible effects on DC. Further clinical and preclinical trials will be needed before making definitive statements. Extracting primary blood DC from patients treated with carfilzomib and analysing the viability, phenotype and function could also be a worthwhile avenue of research.

6. Summary

DC are the most potent APC and as such among the most important links between innate and the adaptive immunity. This is in part due to their unique ability to cross-present via MHC I and MHC II and prime naive $CD8^+$ T cells with co-stimulatory molecules. Their abilities are vital for their use in the development of therapeutic vaccines. Carfilzomib is a second-generation proteasome inhibitor used for treatment of multiple myeloma. With multiple myeloma being incurable, achieving remission combining carfilzomib with long lasting disease control via well tolerated antigen-specific tumour vaccines could be an alternative. In the present work MoDC were generated *in vitro* and cell viability assays were used to determine a suitable dosage for MoDC functional analysis and for determining whether the chosen dosage of 100 nM had enough *in vitro* anti-myeloma effect. The phenotype of the MoDC was analysed by fluorescent antibody labeling for several surface molecules and analysis via flow cytometry. In mMoDC, carfilzomib caused a statistically significant decrease in CD80 and CD83 expression. Bortozomib caused a down-regulation of all analysed surface molecules except CD14 and osteoactivin. In immature imMoDC, carfilzomib caused a statistically significant up-regulation of CD80, bortezomib caused a statistically significant up-regulation of CD83. This suggests carfilzomib having little effect on the phenotype of immature as well as LPS matured mMoDC. Migratory function was measured by cell migration through a porous membrane. Carfilzomib, as opposed to bortezomib, did not significantly reduce *in vitro* migratory function of mMoDC. Cytokine secretion was analysed in ELISA assays of cell-deprived cell culture fluid. Carfilzomib appears to affect mMoDC cytokine production less than bortezomib which caused a statistically significant decrease in imMoDC MCP-1/CCL2 concentration and mMoDC MIP-1α/CCL3 concentration while non-significant results showed a consistent trend of a more pronounced decrease in cytokine concentration in bortezomib than in carfilzomib. Our results suggest carfilzomib only having minor effects on MoDC phenotype and function and it therefore being better suited for combination with tumour vaccination. However, more functional analyses will be needed to support this claim.

7. German Summary

Dendritische Zellen (DC) sind die potentesten antigenpräsentierenden Zellen und somit wichtige Vermittler der Kommunikation von angeborenem und adaptivem Immunsystem. Grund hierfür ist u. a. die einzigartige Fähigkeit, aufgenommene und prozessierte Antigene auf MHC I und MHC II zu präsentieren und die Fähigkeit, naive $CD8^+$ T-Zellen mit kostimulatorischen Oberflächenrezeptoren zu primen. Carfilzomib ist ein Proteasominhibitor der zweiten Generation und für die Therapie des multiplen Myeloms zugelassen, welches in den meisten Fällen nicht heilbar ist. Diese Arbeit sollte den Effekt von Carfilzomib auf *in vitro* aus Monozyten generierten dendritischen Zellen (MoDC), welche in einigen Tumor-Impfungen Anwendung finden, analysieren. Der MoDC-Phänotyp wurde durch Färben mit fluoreszenzmarkierten Antikörpern gegen verschiedene Oberflächenmoleküle und anschließende Messung am Durchflusszytometer bestimmt. Bei reifen MoDC verursachte Carfilzomib eine statistisch signifikante, weniger als bei Bortezomib ausgeprägte Herabregulation von CD80 und CD83. Bortezomib verursachte bei reifen MoDC eine Herabregulation aller Oberflächenmoleküle außer CD14 und Osteoaktivin. Bei unreifen MoDC verursachte Carfilzomib eine statistisch signifikante Hochregulation von CD80 und Bortezomib eine statistisch signifikante Hochregulation von CD83. Dies legt nahe, dass Carfilzomib den Phänotyp nur geringfügig verändert. Die Zellmigration durch eine poröse Membran zeigte keine signifikante Verschlechterung. Die Zytokinsekretion wurde durch ELISAs aus zellfreier Zellkulturflüssigkeit bestimmt. In der Bortezomib Gruppe wurde bei unreifen MoDC eine signifikant geringere Durchschnittskonzentration von MCP-1/CCL2, bei reifen MoDC eine signifikant geringere MIP-1α/CCL3 Konzentration gemessen. Bei allen anderen Zytokinen zeigte sich als Trend, dass Bortezomib einen ausgeprägteren Zytokinkonzentrationsabfall verursachte als Carfilzomib. Diese Ergebnisse suggerieren, dass Carfilzomib sich zur therapeutischen Kombination mit Tumorvakzinen besser eignet als sein Vorgänger Bortezomib.

8. References

1. Aderem A. Phagocytosis and the Inflammatory Response. J Infect Dis. 2003 Jun 15;187(s2):S340–5.
2. Mold C, Gewurz H, Du Clos TW. Regulation of complement activation by C-reactive protein. Immunopharmacology. 1999 May;42(1–3):23–30.
3. Villadangos JA, Schnorrer P. Intrinsic and cooperative antigen-presenting functions of dendritic-cell subsets in vivo. Nat Rev Immunol. 2007 Jul;7(7):543–55.
4. Gelman JS, Sironi J, Berezniuk I, Dasgupta S, Castro LM, Gozzo FC, et al. Alterations of the Intracellular Peptidome in Response to the Proteasome Inhibitor Bortezomib. Gartel AL, editor. PLoS ONE. 2013 Jan 7;8(1):e53263.
5. Bachem A, Güttler S, Hartung E, Ebstein F, Schaefer M, Tannert A, et al. Superior antigen cross-presentation and XCR1 expression define human CD11c+CD141+ cells as homologues of mouse CD8+ dendritic cells. J Exp Med. 2010 Jun 7;207(6):1273–81.
6. Poulin LF, Salio M, Griessinger E, Anjos-Afonso F, Craciun L, Chen J-L, et al. Characterization of human DNGR-1+ BDCA3+ leukocytes as putative equivalents of mouse CD8alpha+ dendritic cells. J Exp Med. 2010 Jun 7;207(6):1261–71.
7. Schroder K, Hertzog PJ, Ravasi T, Hume DA. Interferon-gamma: an overview of signals, mechanisms and functions. J Leukoc Biol. 2004 Feb;75(2):163–89.
8. Slavik JM, Hutchcroft JE, Bierer BE. CD28/CTLA-4 and CD80/CD86 families: signaling and function. Immunol Res. 1999;19(1):1–24.
9. Crotty S. Follicular helper CD4 T cells (TFH). Annu Rev Immunol. 2011;29:621–63.
10. Crotty S. A brief history of T cell help to B cells. Nat Rev Immunol. 2015 Mar;15(3):185–9.
11. Chávez-Galán L, Arenas-Del Angel MC, Zenteno E, Chávez R, Lascurain R. Cell death mechanisms induced by cytotoxic lymphocytes. Cell Mol Immunol. 2009 Feb;6(1):15–25.
12. Paulsen M, Janssen O. Pro- and anti-apoptotic CD95 signaling in T cells. Cell Commun Signal CCS. 2011 Apr 8;9:7.
13. Steinman RM, Cohn ZA. Identification of a novel cell type in peripheral lymphoid organs of mice. I. Morphology, quantitation, tissue distribution. J Exp Med. 1973 May 1;137(5):1142–62.
14. Banchereau J, Steinman RM. Dendritic cells and the control of immunity. Nature. 1998 Mar 19;392(6673):245–52.
15. Aerts-Toegaert C, Heirman C, Tuyaerts S, Corthals J, Aerts JL, Bonehill A, et al. CD83 expression on dendritic cells and T cells: correlation with effective immune responses. Eur J Immunol. 2007 Mar;37(3):686–95.
16. Banchereau J, Briere F, Caux C, Davoust J, Lebecque S, Liu YJ, et al. Immunobiology of dendritic cells. Annu Rev Immunol. 2000;18:767–811.
17. Berard F, Blanco P, Davoust J, Neidhart-Berard EM, Nouri-Shirazi M, Taquet N, et al. Cross-priming of naive CD8 T cells against melanoma antigens using dendritic cells loaded with killed allogeneic melanoma cells. J Exp Med. 2000 Dec 4;192(11):1535–44.

18. Tarbell KV, Yamazaki S, Olson K, Toy P, Steinman RM. CD25+ CD4+ T cells, expanded with dendritic cells presenting a single autoantigenic peptide, suppress autoimmune diabetes. J Exp Med. 2004 Jun 7;199(11):1467–77.
19. McKenna K, Beignon A-S, Bhardwaj N. Plasmacytoid dendritic cells: linking innate and adaptive immunity. J Virol. 2005 Jan;79(1):17–27.
20. Gabrilovich D. Mechanisms and functional significance of tumour-induced dendritic-cell defects. Nat Rev Immunol. 2004 Dec;4(12):941–52.
21. Hanahan D, Weinberg RA. The hallmarks of cancer. Cell. 2000 Jan 7;100(1):57–70.
22. Hanahan D, Weinberg RA. Hallmarks of cancer: the next generation. Cell. 2011 Mar 4;144(5):646–74.
23. Vinay DS, Ryan EP, Pawelec G, Talib WH, Stagg J, Elkord E, et al. Immune evasion in cancer: Mechanistic basis and therapeutic strategies. Semin Cancer Biol. 2015 Dec;35 Suppl:S185–98.
24. Maeda H, Shiraishi A. TGF-beta contributes to the shift toward Th2-type responses through direct and IL-10-mediated pathways in tumor-bearing mice. J Immunol Baltim Md 1950. 1996 Jan 1;156(1):73–8.
25. Palucka K, Banchereau J. Cancer immunotherapy via dendritic cells. Nat Rev Cancer. 2012 Mar 22;12(4):265–77.
26. Filipazzi P, Pilla L, Mariani L, Patuzzo R, Castelli C, Camisaschi C, et al. Limited Induction of Tumor Cross-Reactive T Cells without a Measurable Clinical Benefit in Early Melanoma Patients Vaccinated with Human Leukocyte Antigen Class I-Modified Peptides. Clin Cancer Res. 2012 Dec 1;18(23):6485–96.
27. Leffers N, Lambeck AJA, Gooden MJM, Hoogeboom B-N, Wolf R, Hamming IE, et al. Immunization with a P53 synthetic long peptide vaccine induces P53-specific immune responses in ovarian cancer patients, a phase II trial. Int J Cancer. 2009 Nov 1;125(9):2104–13.
28. Walter S, Weinschenk T, Stenzl A, Zdrojowy R, Pluzanska A, Szczylik C, et al. Multipeptide immune response to cancer vaccine IMA901 after single-dose cyclophosphamide associates with longer patient survival. Nat Med. 2012 Aug;18(8):1254-61.
29. Hu Z, Ott PA, Wu CJ. Towards personalized, tumour-specific, therapeutic vaccines for cancer. Nat Rev Immunol. 2018 Mar;18(3):168–82.
30. Kwak LW, Campbell MJ, Czerwinski DK, Hart S, Miller RA, Levy R. Induction of immune responses in patients with B-cell lymphoma against the surface-immunoglobulin idiotype expressed by their tumors. N Engl J Med. 1992 Oct 22;327(17):1209–15.
31. Schuster SJ, Neelapu SS, Gause BL, Janik JE, Muggia FM, Gockerman JP, et al. Vaccination with patient-specific tumor-derived antigen in first remission improves disease-free survival in follicular lymphoma. J Clin Oncol Off J Am Soc Clin Oncol. 2011 Jul 10;29(20):2787–94.
32. Fritsch EF, Rajasagi M, Ott PA, Brusic V, Hacohen N, Wu CJ. HLA-binding properties of tumor neoepitopes in humans. Cancer Immunol Res. 2014 Jun;2(6):522–9.
33. Yarchoan M, Johnson BA, Lutz ER, Laheru DA, Jaffee EM. Targeting neoantigens to augment antitumour immunity. Nat Rev Cancer. 2017;17(4):209–22.

34. Dubensky TW, Reed SG. Adjuvants for cancer vaccines. Semin Immunol. 2010 Jun;22(3):155–61.
35. Coffman RL, Sher A, Seder RA. Vaccine adjuvants: putting innate immunity to work. Immunity. 2010 Oct 29;33(4):492–503.
36. Santos PM, Butterfield LH. Dendritic Cell–Based Cancer Vaccines. J Immunol. 2018 Jan 15;200(2):443–9.
37. Rosenblatt J, Vasir B, Uhl L, Blotta S, Macnamara C, Somaiya P, et al. Vaccination with dendritic cell/tumor fusion cells results in cellular and humoral antitumor immune responses in patients with multiple myeloma. Blood. 2011 Jan 13;117(2):393–402.
38. Jung S-H, Lee H-J, Lee Y-K, Yang D-H, Kim H-J, Rhee JH, et al. A phase I clinical study of autologous dendritic cell therapy in patients with relapsed or refractory multiple myeloma. Oncotarget. 2017 Jun 20;8(25):41538–48.
39. Lacy MQ, Mandrekar S, Dispenzieri A, Hayman S, Kumar S, Buadi F, et al. Idiotype-pulsed antigen-presenting cells following autologous transplantation for multiple myeloma may be associated with prolonged survival. Am J Hematol. 2009 Dec;84(12):799–802.
40. Rosenblatt J, Avivi I, Vasir B, Uhl L, Munshi NC, Katz T, et al. Vaccination with dendritic cell/tumor fusions following autologous stem cell transplant induces immunologic and clinical responses in multiple myeloma patients. Clin Cancer Res Off J Am Assoc Cancer Res. 2013 Jul 1;19(13):3640–8.
41. Palucka AK, Ueno H, Connolly J, Kerneis-Norvell F, Blanck J-P, Johnston DA, et al. Dendritic cells loaded with killed allogeneic melanoma cells can induce objective clinical responses and MART-1 specific CD8+ T-cell immunity. J Immunother Hagerstown Md 1997. 2006 Oct;29(5):545–57.
42. Kantoff PW, Higano CS, Shore ND, Berger ER, Small EJ, Penson DF, et al. Sipuleucel-T Immunotherapy for Castration-Resistant Prostate Cancer. N Engl J Med. 2010 Jul 29;363(5):411–22.
43. Li D, Romain G, Flamar A-L, Duluc D, Dullaers M, Li X-H, et al. Targeting self- and foreign antigens to dendritic cells via DC-ASGPR generates IL-10-producing suppressive CD4+ T cells. J Exp Med. 2012 Jan 16;209(1):109–21.
44. Landgren O, Kyle RA, Pfeiffer RM, Katzmann JA, Caporaso NE, Hayes RB, et al. Monoclonal gammopathy of undetermined significance (MGUS) consistently precedes multiple myeloma: a prospective study. Blood. 2009 May 28;113(22):5412–7.
45. Palumbo A, Avet-Loiseau H, Oliva S, Lokhorst HM, Goldschmidt H, Rosinol L, et al. Revised International Staging System for Multiple Myeloma: A Report From International Myeloma Working Group. J Clin Oncol. 2015 Sep 10;33(26):2863–9.
46. Siegel RL, Miller KD, Jemal A. Cancer statistics, 2015. CA Cancer J Clin. 2015 Feb;65(1):5–29.
47. Cancer Stat Facts: Myeloma [Internet]. [cited 2018 Mar 21]: https://seer.cancer.gov/statfacts/html/mulmy.html
48. Attal M, Harousseau JL, Stoppa AM, Sotto JJ, Fuzibet JG, Rossi JF, et al. A prospective, randomized trial of autologous bone marrow transplantation and chemotherapy in multiple myeloma. Intergroupe Français du Myélome. N Engl J Med. 1996 Jul 11;335(2):91–7.

49. Roehnisch T, Then C, Nagel W, Blumenthal C, Braciak T, Donzeau M, et al. Phage idiotype vaccination: first phase I/II clinical trial in patients with multiple myeloma. J Transl Med. 2014 May 9;12:119.
50. FDA Approval for Bortezomib [Internet]. [cited 2018 Mar 21]: https://www.cancer.gov/about-cancer/treatment/drugs/fda-bortezomib
51. Bonvini P, Zorzi E, Basso G, Rosolen A. Bortezomib-mediated 26S proteasome inhibition causes cell-cycle arrest and induces apoptosis in CD-30+ anaplastic large cell lymphoma. Leukemia. 2007 Apr;21(4):838–42.
52. Moreau P, Pylypenko H, Grosicki S, Karamanesht I, Leleu X, Grishunina M, et al. Subcutaneous versus intravenous administration of bortezomib in patients with relapsed multiple myeloma: a randomised, phase 3, non-inferiority study. Lancet Oncol. 2011 May;12(5):431–40.
53. Jagannath S, Durie BGM, Wolf JL, Camacho ES, Irwin D, Lutzky J, et al. Extended follow-up of a phase 2 trial of bortezomib alone and in combination with dexamethasone for the frontline treatment of multiple myeloma. Br J Haematol. 2009 Sep;146(6):619–26.
54. Fu W, Delasalle K, Wang J, Song S, Hou J, Alexanian R, et al. Bortezomib-cyclophosphamide-dexamethasone for relapsing multiple myeloma. Am J Clin Oncol. 2012 Dec;35(6):562–5.
55. FDA Approval for Carfilzomib [Internet]. [cited 2018 Mar 21]: https://www.cancer.gov/about-cancer/treatment/drugs/fda-carfilzomib
56. Siegel DS, Martin T, Wang M, Vij R, Jakubowiak AJ, Lonial S, et al. A phase 2 study of single-agent carfilzomib (PX-171-003-A1) in patients with relapsed and refractory multiple myeloma. Blood. 2012 Oct 4;120(14):2817–25.
57. Carfilzomib (Code C52196) NCIthesaurus. In [cited 2018 Mar 21]. Available from: https://ncit.nci.nih.gov/ncitbrowser/pages/concept_details.jsf?dictionary=NCI_Thesaurus&version=16.04d&code=C52196&ns=NCI_Thesaurus&type=properties&key=null&b=1&n=0&vse=null
58. Kuhn DJ, Chen Q, Voorhees PM, Strader JS, Shenk KD, Sun CM, et al. Potent activity of carfilzomib, a novel, irreversible inhibitor of the ubiquitin-proteasome pathway, against preclinical models of multiple myeloma. Blood. 2007 Nov 1;110(9):3281–90.
59. Muchtar E, Gertz MA, Magen H. A practical review on carfilzomib in multiple myeloma. Eur J Haematol. 2016 Jun;96(6):564–77.
60. Stewart AK, Rajkumar SV, Dimopoulos MA, Masszi T, Špička I, Oriol A, et al. Carfilzomib, Lenalidomide, and Dexamethasone for Relapsed Multiple Myeloma. N Engl J Med. 2015 Jan 8;372(2):142–52.
61. Dimopoulos MA, Moreau P, Palumbo A, Joshua D, Pour L, Hájek R, et al. Carfilzomib and dexamethasone versus bortezomib and dexamethasone for patients with relapsed or refractory multiple myeloma (ENDEAVOR): a randomised, phase 3, open-label, multicentre study. Lancet Oncol. 2016 Jan;17(1):27–38.
62. Bensinger WI, Maloney D, Storb R. Allogeneic hematopoietic cell transplantation for multiple myeloma. Semin Hematol. 2001 Jul;38(3):243–9.

63. Schwarz K, de Giuli R, Schmidtke G, Kostka S, van den Broek M, Kim KB, et al. The selective proteasome inhibitors lactacystin and epoxomicin can be used to either up- or down-regulate antigen presentation at nontoxic doses. J Immunol Baltim Md 1950. 2000 Jun 15;164(12):6147–57.
64. Nencioni A, Garuti A, Schwarzenberg K, Cirmena G, Dal Bello G, Rocco I, et al. Proteasome inhibitor-induced apoptosis in human monocyte-derived dendritic cells. Eur J Immunol. 2006 Mar;36(3):681–9.
65. Nencioni A, Schwarzenberg K, Brauer KM, Schmidt SM, Ballestrero A, Grünebach F, et al. Proteasome inhibitor bortezomib modulates TLR4-induced dendritic cell activation. Blood. 2006 Jul 15;108(2):551–8.
66. Leone P, Berardi S, Frassanito MA, Ria R, De Re V, Cicco S, et al. Dendritic cells accumulate in the bone marrow of myeloma patients where they protect tumor plasma cells from CD8+ T-cell killing. Blood. 2015 Sep 17;126(12):1443–51.
67. Walz S, Stickel JS, Kowalewski DJ, Schuster H, Weisel K, Backert L, et al. The antigenic landscape of multiple myeloma: mass spectrometry (re)defines targets for T-cell-based immunotherapy. Blood. 2015 Sep 3;126(10):1203–13.
68. Kowalewski DJ, Walz S, Backert L, Schuster H, Kohlbacher O, Weisel K, et al. Carfilzomib alters the HLA-presented peptidome of myeloma cells and impairs presentation of peptides with aromatic C-termini. Blood Cancer J. 2016 Apr;6(4):e411–e411.
69. Romani N, Reider D, Heuer M, Ebner S, Kämpgen E, Eibl B, et al. Generation of mature dendritic cells from human blood. An improved method with special regard to clinical applicability. J Immunol Methods. 1996 Sep 27;196(2):137–51.
70. Sallusto F, Lanzavecchia A. Efficient presentation of soluble antigen by cultured human dendritic cells is maintained by granulocyte/macrophage colony-stimulating factor plus interleukin 4 and downregulated by tumor necrosis factor alpha. J Exp Med. 1994 Apr 1;179(4):1109–18.
71. Caux C, Massacrier C, Vanbervliet B, Barthelemy C, Liu YJ, Banchereau J. Interleukin 10 inhibits T cell alloreaction induced by human dendritic cells. Int Immunol. 1994 Aug;6(8):1177–85.
72. Corinti S, Albanesi C, la Sala A, Pastore S, Girolomoni G. Regulatory activity of autocrine IL-10 on dendritic cell functions. J Immunol Baltim Md 1950. 2001 Apr 1;166(7):4312–8.
73. Demo SD, Kirk CJ, Aujay MA, Buchholz TJ, Dajee M, Ho MN, et al. Antitumor activity of PR-171, a novel irreversible inhibitor of the proteasome. Cancer Res. 2007 Jul 1;67(13):6383–91.
74. Wang Z, Yang J, Kirk C, Fang Y, Alsina M, Badros A, et al. Clinical Pharmacokinetics, Metabolism, and Drug-Drug Interaction of Carfilzomib. Drug Metab Dispos. 2013 Jan 1;41(1):230–7.
75. Castiello L, Sabatino M, Jin P, Clayberger C, Marincola FM, Krensky AM, et al. Monocyte-derived DC maturation strategies and related pathways: a transcriptional view. Cancer Immunol Immunother. 2011 Apr;60(4):457–66.

76. Vermes I, Haanen C, Steffens-Nakken H, Reutelingsperger C. A novel assay for apoptosis. Flow cytometric detection of phosphatidylserine expression on early apoptotic cells using fluorescein labelled Annexin V. J Immunol Methods. 1995 Jul 17;184(1):39–51.
77. Nicoletti I, Migliorati G, Pagliacci MC, Grignani F, Riccardi C. A rapid and simple method for measuring thymocyte apoptosis by propidium iodide staining and flow cytometry. J Immunol Methods. 1991 Jun 3;139(2):271–9.
78. Knödler A, Schmidt SM, Bringmann A, Weck MM, Brauer KM, Holderried T a. W, et al. Post-transcriptional regulation of adapter molecules by IL-10 inhibits TLR-mediated activation of antigen-presenting cells. Leukemia. 2009 Mar;23(3):535–44.
79. Cernadas M, Lu J, Watts G, Brenner MB. CD1a expression defines an interleukin-12 producing population of human dendritic cells. Clin Exp Immunol. 2009 Mar;155(3):523-33.
80. van Kooyk Y, Geijtenbeek TBH. DC-SIGN: escape mechanism for pathogens. Nat Rev Immunol. 2003 Sep;3(9):697–709.
81. Ohl L, Mohaupt M, Czeloth N, Hintzen G, Kiafard Z, Zwirner J, et al. CCR7 governs skin dendritic cell migration under inflammatory and steady-state conditions. Immunity. 2004 Aug;21(2):279–88.
82. Schwarzbich M-A, Gutknecht M, Salih J, Salih HR, Brossart P, Rittig SM, et al. The immune inhibitory receptor osteoactivin is upregulated in monocyte-derived dendritic cells by BCR-ABL tyrosine kinase inhibitors. Cancer Immunol Immunother CII. 2012 Feb;61(2):193–202.
83. Hilkens CM, Kalinski P, de Boer M, Kapsenberg ML. Human dendritic cells require exogenous interleukin-12-inducing factors to direct the development of naive T-helper cells toward the Th1 phenotype. Blood. 1997 Sep 1;90(5):1920–6.
84. Dudek AM, Martin S, Garg AD, Agostinis P. Immature, Semi-Mature, and Fully Mature Dendritic Cells: Toward a DC-Cancer Cells Interface That Augments Anticancer Immunity. Front Immunol. 2013 Dec 11;4:438.
85. Gonzalez-Quesada C, Frangogiannis NG. Monocyte chemoattractant protein-1/CCL2 as a biomarker in acute coronary syndromes. Curr Atheroscler Rep. 2009 Mar;11(2):131–8.
86. Ajuebor MN, Kunkel SL, Hogaboam CM. The role of CCL3/macrophage inflammatory protein-1alpha in experimental colitis. Eur J Pharmacol. 2004 Aug 30;497(3):343–9.
87. Suffee N, Richard B, Hlawaty H, Oudar O, Charnaux N, Sutton A. Angiogenic properties of the chemokine RANTES/CCL5. Biochem Soc Trans. 2011 Dec;39(6):1649-53.
88. Jones SA. Directing transition from innate to acquired immunity: defining a role for IL-6. J Immunol Baltim Md 1950. 2005 Sep 15;175(6):3463–8.
89. Vignali DAA, Kuchroo VK. IL-12 family cytokines: immunological playmakers. Nat Immunol. 2012 Jul 19;13(8):722–8.
90. Straube C, Wehner R, Wendisch M, Bornhäuser M, Bachmann M, Rieber EP, et al. Bortezomib significantly impairs the immunostimulatory capacity of human myeloid blood dendritic cells. Leukemia. 2007 Jul;21(7):1464–71.

91. Chang C-L, Hsu Y-T, Wu C-C, Yang Y-C, Wang C, Wu T-C, et al. Immune Mechanism of the Antitumor Effects Generated by Bortezomib. J Immunol. 2012 Sep 15;189(6):3209-20.
92. Zinser E, Rössner S, Littmann L, Lüftenegger D, Schubert U, Steinkasserer A. Inhibition of the proteasome influences murine and human dendritic cell development in vitro and in vivo. Immunobiology. 2009;214(9–10):843–51.
93. Wang Y, Liang Y, Zhang Y, Wu D, Liu H. Bortezomib inhibits bone marrow-derived dendritic cells. Int J Clin Exp Pathol. 2015;8(5):4857–62.
94. Hill L, Alousi A, Kebriaei P, Mehta R, Rezvani K, Shpall E. New and emerging therapies for acute and chronic graft versus host disease. Ther Adv Hematol. 2018 Jan;9(1):21–46.
95. Dall'Era M, Davis J. CTLA4Ig: a novel inhibitor of costimulation. Lupus. 2004;13(5):372–6.
96. NCT03457142 [Internet]: https://clinicaltrials.gov/ct2/show/NCT03457142
97. Murray ME, Gavile CM, Nair JR, Koorella C, Carlson LM, Buac D, et al. CD28-mediated pro-survival signaling induces chemotherapeutic resistance in multiple myeloma. Blood. 2014 Jun 12;123(24):3770–9.
98. Zhang L, Pham LV, Newberry KJ, Ou Z, Liang R, Qian J, et al. In Vitro and In Vivo Therapeutic Efficacy of Carfilzomib in Mantle Cell Lymphoma: Targeting the Immunoproteasome. Mol Cancer Ther. 2013 Nov 1;12(11):2494–504.
99. Busonero C, Leone S, Klemm C, Acconcia F. A functional drug re-purposing screening identifies carfilzomib as a drug preventing 17β-estradiol: ERα signaling and cell proliferation in breast cancer cells. Mol Cell Endocrinol. 2018 Jan 15;460:229–37.
100. Thaler S, Schmidt M, Roβwag S, Thiede G, Schad A, Sleeman JP. Proteasome inhibitors prevent bi-directional HER2/estrogen-receptor cross-talk leading to cell death in endocrine and lapatinib-resistant HER2+/ER+ breast cancer cells. Oncotarget. 2017 Sep 22;8(42):72281–301.
101. Shi Y, Yu Y, Wang Z, Wang H, Bieerkehazhi S, Zhao Y, et al. Second-generation proteasome inhibitor carfilzomib enhances doxorubicin-induced cytotoxicity and apoptosis in breast cancer cells. Oncotarget. 2016 08;7(45):73697–710.
102. Mehta A, Zhang L, Boufraqech M, Zhang Y, Patel D, Shen M, et al. Carfilzomib is an effective anticancer agent in anaplastic thyroid cancer. Endocr Relat Cancer. 2015 Jun;22(3):319–29.
103. Baker AF, Hanke NT, Sands BJ, Carbajal L, Anderl JL, Garland LL. Carfilzomib demonstrates broad anti-tumor activity in pre-clinical non-small cell and small cell lung cancer models. J Exp Clin Cancer Res CR. 2014 Dec 31;33:111.
104. Forsythe N, Refaat A, Javadi A, Khawaja H, Weir J-A, Emam H, et al. The unfolded protein response: a novel therapeutic target for poor prognostic BRAF mutant colorectal cancer. Mol Cancer Ther. 2018 Feb 26;molcanther.0603.2017.
105. Ao L, Reichel D, Hu D, Jeong H, Kim KB, Bae Y, et al. Polymer micelle formulations of proteasome inhibitor carfilzomib for improved metabolic stability and anticancer efficacy in human multiple myeloma and lung cancer cell lines. J Pharmacol Exp Ther. 2015 Nov;355(2):168–73.

106. Zhang L, Yang X, Sun Z, Li J, Zhu H, Li J, et al. Dendritic cell vaccine and cytokine-induced killer cell therapy for the treatment of advanced non-small cell lung cancer. Oncol Lett. 2016 Apr;11(4):2605–10.
107. Lee H-M, Lee E, Yeo S-Y, Shin S, Park H-K, Nam D-H, et al. Drug repurposing screening identifies bortezomib and panobinostat as drugs targeting cancer associated fibroblasts (CAFs) by synergistic induction of apoptosis. Invest New Drugs [Internet]. 2018 Jan 18 [cited 2018 Mar 29]: http://link.springer.com/10.1007/s10637-017-0547-8

9. List of Tables

10. List of Figures

11. List of Abbreviations

ASGPR	Asialoglycoprotein Receptor
APC	Antigen-prensenting Cell / Allophycocyanin (FACS)
BSA	Bovine Serum Albumin
CCL	Chemokine Ligand
CCR	Chemokine Receptor
CD	Cluster(s) of Differentiation
CD40L	CD40 Ligand
CTL	Cytotoxic T Lymphocyte(s)
DC	Dendritic Cell
i/mDC	Immature/Mature Dendritic Cell(s)
MoDC	Monocyte-Derived Dendritic Cell(s)
imMoDC	Immature Monocyte-Derived Dendritic Cell(s)
mMoDC	Mature Monocyte-Derived Dendritic Cell(s)
DMSO	Dimethylsulfoxid
DNA	Desoxyribonucleic Acid
FACS	Fluorescence-Activated Cell Sorter
FCS	Fetal Calf Serum
FDA	Food and Drug Administration
FITC	Fluorescein Isothiocyanate
FSC	Forward Scatter
GM-CSF	Granulocyte-Macrophage-Colony Stimulating Factor
HER2	Human Epidermal Growth Factor 2
HLA-DR	Human Leukocyte Antigen-Antigen D Related
HPC	Hematopoietic Progenitor Cells
Ig	Immunoglobulin
IL	Interleukin
iMC	Immature Myeloid Cell
LDL	Low-Densitiy Lipoprotein

LDH	Lactate Dehydrogenase
LPS	Lipopolysaccharid
MGUS	Monoclonal Gammopathy of Undetermined Significance
MHC I / II	Major Histocompability Complex I / II
MAP	Mitogen Activated Protein
MCP	Monocyte Chemotactic Protein
MIP	Macrophage Inflammatory Protein
MYD88	Myeloid Differentiation Primary Response 88
NF	Nuclear Factor
PAMP	Pathogen-associated Molecular Pattern
PBMC	Peripheral Blood Mononuclear Cell
PBS	Phosphate Buffered Saline
PE	Phycoerythrin
PerCP	Peridinin-Chlorophyll-Protein Complex
PI3-K	Phosphatidyl-Inositol-3-Kinase
PRR	Pattern Recognation Receptor
PSA	Prostate Specific Antigen
RANTES	Regulated on Activation, Normal T Cell Expressed and Secreted
RNA	Ribonucleic Acid
SSC	Side Scatter
TCR	T Cell Receptor
T_{fh} Cell	T Follicular Helper Cell
T_h Cell	T Helper Cell
T_{reg} Cell	Regulatory T Cell
TGF	Transforming Growth Factor
TLR	Toll-Like Receptor
TLR-L	Toll-Like Receptor Ligand
TNF	Tumour Necrosis Factor

12. Erklärung zum Eigenanteil der Dissertationsschrift

Die Arbeit wurde in der medizinischen Universitätsklinik Tübingen, AG Experimentelle Immuntherapie unter Betreuung von PD Dr. rer. nat. Frank Grünebach durchgeführt.

Die Konzeption der Studie erfolgte durch Dr. med. Susanne M. Rittig, Dr. med. Daniela Dörfel und Dr. rer. nat. Frank Grünebach.

Die ELISA und Annexin-V-Fluoscein / PI Methode wurde durch Sylvia Klein durchgeführt. Die anderen Versuche wurden nach Einarbeitung durch Sylvia Klein von mir eigenständig durchgeführt.

Die statistische Auswertung erfolgte eigenständig durch mich.

Die Betreuung der Arbeit erfolgte durch Dr. med. Susanne M. Rittig, Dr. med. Daniela Dörfel und Dr. rer. nat. Frank Grünebach. Die Korrektur der Arbeit erfolgte durch Dr. med. Susanne Rittig und PD Dr. rer. nat. Frank Grünebach.

Ich versichere, das Manuskript selbständig verfasst zu haben und keine weiteren als die von mir angegebenen Quellen verwendet zu haben.

Hamm, den 21.06.2019

Marius Dahlfrancis

13. Danksagung

Zuerst möchte ich meinem Doktorvater PD Dr. rer. nat. Frank Grünebach dafür danken, dass er mir diese Doktorarbeit unter seiner Führung ermöglicht hat.

Auch bedanke ich mich bei Dr. med. Susanne Rittig und Dr. med. Daniela Dörfel für die persönliche Betreuung während des Projekts.

Besonderer Dank gilt auch Frau Sylvia Klein, die trotz Verpflichtungen in der universitären Kinderklinik viel Zeit und Geduld für meine Einarbeitung aufbrachte. Ohne ihre Mithilfe wäre diese Arbeit nicht möglich gewesen.

Ich möchte mich bei allen Mitarbeitern im Labor, sowohl für das angenehme Arbeitsklima und die kleinen Ratschläge mit großer Wirkung bedanken, als auch für die nette Zeit außerhalb des Labors und auf der DGHO Tagung in Basel.

Meiner Mutter danke ich für ihre jahrzehntelangen Bemühungen, meine Arbeitseffizienz von zu langsam auf adäquat zu steigern und natürlich für ihre moralische Unterstützung während meiner gesamten Ausbildung.

Meiner Taufpatin Margret Juchmann möchte ich ebenfalls für die moralische Unterstützung und die stets ermutigenden Worte danken.

Meinem Bruder danke ich von ganzem Herzen für das professionelle Korrekturlesen und nützliche Tipps wie z. B. den Speed Reader.

Zuletzt danke ich natürlich auch allen lieben Menschen aus meinem Freundeskreis, die ein wichtiges Gegengewicht zu den Stressoren des Projekts und anderen Verpflichtungen schafften und schaffen.